

Synthesis and Second-Order Nonlinear Optical Properties of Donor–Acceptor σ -Alkynyl and σ -Enynyl Indenylruthenium(II) Complexes. X-ray Crystal Structures of

$[\text{Ru}\{\text{C}\equiv\text{CCH}=\text{C}(\text{C}_6\text{H}_4\text{NO}_2\text{-3})_2\}(\eta^5\text{-C}_9\text{H}_7)(\text{PPh}_3)_2]$ and $(EE)\text{-}[\text{Ru}\{\text{C}\equiv\text{C}(\text{CH}=\text{CH})_2\text{-C}_6\text{H}_4\text{NO}_2\text{-4}\}(\eta^5\text{-C}_9\text{H}_7)(\text{PPh}_3)_2]$

Victorio Cadierno, Salvador Conejero, M. Pilar Gamasa, and José Gimeno*,†

Departamento de Química Orgánica e Inorgánica, Instituto Universitario de Química Organometálica “Enrique Moles” (Unidad Asociada al CSIC), Facultad de Química, Universidad de Oviedo, E-33071 Oviedo, Spain

Inge Asselberghs, Stephan Houbrechts,‡ Koen Clays, and André Persoons

Laboratory of Chemical and Biological Dynamics, Center for Research on Molecular Electronics and Photonics, University of Leuven, B-3001 Leuven, Belgium

Javier Borge and Santiago García-Granda

Departamento de Química Física y Analítica, Facultad de Química, Universidad de Oviedo, E-33071 Oviedo, Spain

Received August 5, 1998

σ -Alkynyl complexes $[\text{Ru}(\text{C}\equiv\text{C}-\text{C}_6\text{H}_4\text{R-4})(\eta^5\text{-C}_9\text{H}_7)\text{L}_2]$ ($\text{L} = \text{PPh}_3$, $\text{R} = \text{NO}_2$ (**3a**), $\text{C}\equiv\text{C}-\text{C}_6\text{H}_4\text{-NO}_2\text{-4}$ (**4**), $\text{N}=\text{CH}-\text{C}_6\text{H}_4\text{NO}_2\text{-4}$ (**5**); $\text{L}_2 = 1,2\text{-bis}(\text{diphenylphosphino})\text{ethane}$ (dppe), $\text{R} = \text{NO}_2$ (**3b**); $\text{L}_2 = \text{bis}(\text{diphenylphosphino})\text{methane}$ (dppm), $\text{R} = \text{NO}_2$ (**3c**)) have been prepared by reaction of $[\text{RuCl}(\eta^5\text{-C}_9\text{H}_7)\text{L}_2]$ (**1a–c**) with $\text{HC}\equiv\text{C}-\text{C}_6\text{H}_4\text{R-4}$ and NaPF_6 , via deprotonation of the corresponding intermediate vinylidene derivatives. The treatment of the alkynyl–phosphonio complex $[\text{Ru}\{\text{C}\equiv\text{CCH}_2(\text{PPh}_3)\}(\eta^5\text{-C}_9\text{H}_7)(\text{PPh}_3)_2][\text{PF}_6]$ (**6**) with Li^nBu and the appropriate aldehyde or ketone yields, via Wittig type reactions, σ -enynyl complexes $[\text{Ru}\{\text{C}\equiv\text{CCH}=\text{CR}^1(\text{CH}=\text{CH})_n\text{R}^2\}(\eta^5\text{-C}_9\text{H}_7)(\text{PPh}_3)_2]$ ($n = 0$, $\text{R}^1 = \text{H}$, $\text{R}^2 = \text{C}_6\text{H}_4\text{NO}_2\text{-4}$ (**7a**), $\text{C}_4\text{H}_2\text{ONO}_2\text{-3,4}$ (**8a**), $\text{C}_4\text{H}_2\text{SNO}_2\text{-3,4}$ (**8b**), $\text{C}_6\text{H}_4\text{-CN-4}$ (**13**), $\text{C}_5\text{H}_4\text{N-4}$ (**16**); $n = 0$, $\text{R}^1 = \text{R}^2 = \text{C}_6\text{H}_4\text{NO}_2\text{-3}$ (**9**); $n = 1$, $\text{R}^1 = \text{H}$, $\text{R}^2 = \text{C}_6\text{H}_4\text{NO}_2\text{-4}$ (**7b**)) isolated as mixtures of the corresponding *E* and *Z* stereoisomers. The structures of complexes **7b** and **9** have been confirmed by X-ray diffraction. Structural data in the solid state as well as in solution ($^{13}\text{C}\{^1\text{H}\}$ NMR) show an extensive electronic delocalization between the donor fragment $[\text{Ru}(\eta^5\text{-C}_9\text{H}_7)(\text{PPh}_3)_2]$ and the acceptor nitroaryl group. In accordance with this, values of resonantly enhanced molecular quadratic hyperpolarizabilities (β) for these donor–acceptor derivatives ($\beta_{1064\text{ nm}} = 100\text{--}1320 \times 10^{-30}$ esu), determined by the hyper-Rayleigh scattering technique (HRS) at 1064 nm which are dependent on the molecular design of the bridged enynyl chain, are significantly larger than those of their analogous organic chromophores. Mixed-valence bimetallic donor–acceptor derivatives $[(\eta^5\text{-C}_9\text{H}_7)(\text{PPh}_3)_2\text{Ru}\{\mu\text{-C}\equiv\text{N}\}\text{ML}_5][\text{CF}_3\text{SO}_3]_n$ ($n = 0$, $\text{ML}_5 = \text{Cr}(\text{CO})_5$ (**11a**), $\text{W}(\text{CO})_5$ (**11b**); $n = 3$, $\text{ML}_5 = \text{Ru}(\text{NH}_3)_5$ (**12**)), $[(\eta^5\text{-C}_9\text{H}_7)(\text{PPh}_3)_2\text{Ru}\{\mu\text{-C}\equiv\text{CCH}=\text{CH}-\text{C}_6\text{H}_4\text{C}\equiv\text{N-4}\}\text{ML}_5][\text{CF}_3\text{SO}_3]_n$ ($n = 0$, $\text{ML}_5 = \text{Cr}(\text{CO})_5$ [*E*, *Z*]-**14a**], $\text{W}(\text{CO})_5$ [*E*, *Z*]-**14b**]; $n = 3$, $\text{ML}_5 = \text{Ru}(\text{NH}_3)_5$ [*E*, *Z*]-**15**] and $[(\eta^5\text{-C}_9\text{H}_7)(\text{PPh}_3)_2\text{Ru}\{\mu\text{-C}\equiv\text{CCH}=\text{CH}-\text{C}_5\text{H}_4\text{N-4}\}\text{M}(\text{CO})_5]$ ($\text{M} = \text{Cr}$ [*E*]-**17a**], W [*E*]-**17b**]) have also been prepared in high yields. Static quadratic hyperpolarizabilities values of these derivatives ($\beta_0 = 10\text{--}150 \times 10^{-30}$ esu) surpass the largest reported to date for bimetallic compounds. The bimetallic σ -enynyl complex $[\text{Ru}(\text{C}\equiv\text{CCH}=\text{CH}(\eta^5\text{-C}_5\text{H}_4)\text{Fe}(\eta^5\text{-C}_5\text{H}_5)(\eta^5\text{-C}_9\text{H}_7)(\text{PPh}_3)_2)]$ [*E*]-**18**] was obtained stereoselectively from the alkynyl–phosphonio complex **6**, Li^nBu , and $\{\eta^5\text{-C}_5\text{H}_4(\text{CHO})\}\text{Fe}(\eta^5\text{-C}_5\text{H}_5)$. Protonation of *E*-**18** with HBF_4 yields the vinylidene derivative $[\text{Ru}\{\text{C}=\text{C}(\text{H})\text{CH}=\text{CH}(\eta^5\text{-C}_5\text{H}_4)\text{Fe}(\eta^5\text{-C}_5\text{H}_5)\}(\eta^5\text{-C}_9\text{H}_7)(\text{PPh}_3)_2][\text{BF}_4]$ (**19**). Quadratic hyperpolarizabilities for these ruthenium(II)–iron(II) bimetallic complexes are also reported.

Introduction

The search for suitable materials displaying second-order nonlinear optical (NLO) properties is the focus of

much current research activity due to their potential applications in optoelectronics, telecommunications, and optical storage devices.¹ A great deal of work has been carried out on organic molecules which has enabled the development of certain structure–NLO efficiency relationships. Thus, it is well-known that organic molecules

* E-mail: jgh@sauron.quimica.uniovi.es.

† Present address: Frontier Research Program, RIKEN, 2-1 Hiro-sawa, Wako-shi, Saitama 351-01, Japan.

containing donor–acceptor-substituted π -conjugated systems exhibit large second-order NLO properties.² The optical nonlinearities of organometallic compounds have been actively studied only recently, but their potential as novel NLO materials is yet to be fully explored. Enhanced second-order NLO responses have also been found on organometallic systems with a donor–bridge–acceptor composition.³ In these complexes the metal fragment can act as an electron donor,⁴ as an electron acceptor group,⁵ or as part of a polarizable bridge.⁶ Moreover, the incorporation of the metal in the same plane as the π -conjugated system and the potential introduction of metal–carbon multiple-bond character has been suggested to enhance the NLO response.^{4c} Attention has turned to σ -alkynyl complexes which certainly satisfy this molecular design. In this respect, Humphrey et al. have reported the extremely large molecular second-order responses of several 18 valence electron ruthenium(II)⁷ and nickel(II)⁸ complexes and 14 valence electron gold(II)⁹ σ -alkynyl derivatives in which the metal fragments act as electron donor groups. The quadratic hyperpolarizabilities (β) of these complexes revealed the second-order NLO series $[\text{Ru}] > [\text{Ni}] > [\text{Au}]$, with a great dependence of the NLO response on the structure and lengthening of the alkynyl skeleton.

During recent years we have been involved in the study of the reactivity of unsaturated carbene complexes containing the electron-rich indenylruthenium(II) moiety $[\text{Ru}(\eta^5\text{-C}_9\text{H}_7)(\text{PPh}_3)_2]$ as a metal auxiliary, and we have described the synthesis of a large variety of functionalized (σ -alkynyl)ruthenium(II) complexes.¹⁰ Since we are specially interested in exploiting the

potential utility of these derivatives, we wondered about the possible effect of this metallic auxiliary on second-order NLO materials. Thus, in this paper we report the synthesis of novel donor–acceptor indenylruthenium(II) complexes which display large quadratic hyperpolarizabilities (β). We have investigated systematically series of compounds of the following types (see Chart 1): (i) σ -alkynyl and σ -enynyl complexes (**A**) containing nitro or cyano substituents at the end of the hydrocarbon chain, (ii) ruthenium(II)–ruthenium(III) and ruthenium(II)–chromium(0) or tungsten(0) bimetallic complexes (**B**) in which a donor indenylruthenium(II) moiety and an acceptor metal fragment are bridged by a cyano group or an enynyl N-functionalized system, and (iii) ruthenium(II)–iron(II) bimetallic complexes (**C**) in which an indenylruthenium(II) moiety and a ferrocenyl fragment are bridged by an enynyl or vinylvinylidene unsaturated chain. Part of this work has been previously communicated.¹¹

Results and Discussion

σ -Alkynyl Donor–Acceptor Complexes $[\text{Ru}(\text{C}\equiv\text{C}-\text{C}_6\text{H}_4\text{NO}_2-4)(\eta^5\text{-C}_9\text{H}_7)\text{L}_2]$ ($\text{L}_2 = 2\text{PPh}_3$ (3a**), **1,2** bis(diphenylphosphino)ethane (dppe) (**3b**), bis(diphenylphosphino)methane (dppm) (**3c**)) and $[\text{Ru}(\text{C}\equiv\text{C}-\text{C}_6\text{H}_4\text{R}-4)(\eta^5\text{-C}_9\text{H}_7)(\text{PPh}_3)_2]$ ($\text{R} = \text{C}\equiv\text{C}-\text{C}_6\text{H}_4\text{NO}_2-4$ (**4**), $\text{N}=\text{CH}-\text{C}_6\text{H}_4\text{NO}_2-4$ (**5**)).** The reaction of complexes $[\text{RuCl}(\eta^5\text{-C}_9\text{H}_7)\text{L}_2]$ ($\text{L}_2 = 2\text{PPh}_3$ (**1a**), dppe (**1b**), dppm (**1c**)) with 4-ethynylnitrobenzene in refluxing methanol, and in the presence of NaPF_6 , results in the formation of the vinylidene complexes $[\text{Ru}\{\text{C}=\text{C}(\text{H})-\text{C}_6\text{H}_4\text{NO}_2-4\}(\eta^5\text{-C}_9\text{H}_7)\text{L}_2][\text{PF}_6]$ (**2a–c**), which have been

(1) (a) Prasad, P. N.; Williams, D. J. *Introduction to Nonlinear Optical Effects in Molecules and Polymers*; Wiley-Interscience: New York, 1991. (b) Boyd, R. W. *Nonlinear Optics*; Academic Press: San Diego, CA, 1992. (c) Zyss, J. *Molecular Nonlinear Optics*; Academic Press: New York, 1994.

(2) For example, see: (a) Williams, D. J. *Angew. Chem., Int. Ed. Engl.* **1984**, *23*, 690 and references therein. (b) Cheng, L.-T.; Tam, W.; Stevenson, S. H.; Meredith, G. R.; Rikken, G.; Marder, S. R. *J. Phys. Chem.* **1991**, *95*, 10631. (c) Cheng, L.-T.; Tam, W.; Marder, S. R.; Stiegman, A. E.; Rikken, G.; Spangler, C. W. *J. Phys. Chem.* **1991**, *95*, 10643.

(3) (a) Nalwa, H. S. *Appl. Organomet. Chem.* **1991**, *5*, 349. (b) Long, N. J. *Angew. Chem., Int. Ed. Engl.* **1995**, *34*, 21. (c) Whittall, I. R.; McDonagh, A. M.; Humphrey, M. G.; Samoc, M. *Adv. Organomet. Chem.* **1998**, *42*, 291. (d) Denning, R. G. *J. Mater. Chem.* **1995**, *5*, 365.

(4) The most extensively studied system is that of ferrocenyl derivatives. For example, see: (a) Green, M. L. H.; Marder, S. R.; Thompson, M. E.; Bandy, J. A.; Bloor, D.; Kolinsky, P. V.; Jones, R. J. *Nature* **1987**, *330*, 360. (b) Tiemann, B. G.; Marder, S. R.; Perry, J. W.; Cheng, L.-T. *Chem. Mater.* **1990**, *2*, 690. (c) Calabrese, J. C.; Cheng, L.-T.; Green, J. C.; Marder, S. R.; Tam, W. *J. Am. Chem. Soc.* **1991**, *113*, 7227. (d) Yuan, Z.; Taylor, N. J.; Sun, Y.; Marder, T. B. *J. Organomet. Chem.* **1993**, *449*, 27. (e) Blanchard-Desce, M.; Runser, C.; Fort, A.; Barzoukas, M.; Lehn, J.-M.; Bloy, V.; Alain, V. *Chem. Phys.* **1995**, *199*, 253. (f) Hagenau, U.; Heck, J.; Hendricks, E.; Persoons, A.; Schuld, T.; Wong, H. *Inorg. Chem.* **1996**, *35*, 7863.

(5) Metal carbonyl fragments have been used as electron-acceptor groups. For example, see: (a) Cheng, L.-T.; Tam, W.; Eaton, D. F. *Organometallics* **1990**, *9*, 2856. (b) Cheng, L.-T.; Tam, W.; Meredith, G. R.; Marder, S. R. *Mol. Cryst. Liq. Cryst.* **1990**, *189*, 137. (c) Maiorana, S.; Papagni, A.; Licandro, E.; Persoons, A.; Clays, K.; Houbrechts, S.; Porzio, W. *Gazz. Chim. Ital.* **1995**, *125*, 377. (d) Lacroix, P. G.; Lin, W.; Wong, G. K. *Chem. Mater.* **1995**, *7*, 1293. (e) Roth, G.; Fischer, H.; Meyer-Friedrichsen, T.; Heck, J.; Houbrechts, S.; Persoons, A. *Organometallics* **1998**, *17*, 1511.

(6) For example, see: (a) LeCours, S. M.; Guan, H.-W.; DiMugno, S. G.; Wang, C. H.; Therien, M. J. *J. Am. Chem. Soc.* **1996**, *118*, 1497. (b) Nguyen, P.; Lesley, G.; Marder, T. B.; Ledoux, I.; Zyss, J. *Chem. Mater.* **1997**, *9*, 406. (c) Karki, L.; Vance, F. W.; Hupp, J. T.; LeCours, S. M.; Therien, M. J. *J. Am. Chem. Soc.* **1998**, *120*, 2606. (d) Buey, J.; Coco, S.; Diez, L.; Espinet, P.; Martín-Alvarez, J. M.; Miguel, J. A.; García-Granda, S.; Tesouro, A.; Ledoux, I.; Zyss, J. *Organometallics* **1998**, *17*, 1750.

(7) $[\text{Ru}(\eta^5\text{-C}_5\text{H}_5)(\text{PR}_3)_2]$: (a) Whittall, I. R.; Humphrey, M. G.; Houbrechts, S.; Persoons, A. *Organometallics* **1996**, *15*, 1935. (b) Naulty, R. H.; Cifuentes, M. P.; Humphrey, M. G.; Houbrechts, S.; Boutton, C.; Persoons, A.; Heath, G. A.; Hockless, D. C. R.; Luther-Davies, B.; Samoc, M. *J. Chem. Soc., Dalton Trans.* **1997**, 4167. (c) Wu, I.-Y.; Lin, J. T.; Luo, J.; Sun, S.-S.; Li, C.-S.; Lin, K. J.; Tsai, C.; Hsu, C.-C.; Lin, J.-L. *Organometallics* **1997**, *16*, 2038. (d) Whittall, I. R.; Cifuentes, M. P.; Humphrey, M. G.; Luther-Davies, B.; Samoc, M.; Houbrechts, S.; Persoons, A.; Heath, G. A.; Hockless, D. C. R. *J. Organomet. Chem.* **1997**, *549*, 127. (e) Wu, I.-Y.; Lin, J. T.; Luo, J.; Li, C.-S.; Tsai, C.; Wen, Y. S.; Hsu, C.-C.; Yeh, F.-F.; Liou, S. *Organometallics* **1998**, *17*, 2188. *trans*- $[\text{RuCl}(\text{dppm})_2]$: (f) Whittall, I. R.; Humphrey, M. G.; Houbrechts, S.; Maes, J.; Persoons, A.; Schmid, S.; Hockless, D. C. R. *J. Organomet. Chem.* **1997**, *544*, 277. (g) Whittall, I. R.; Humphrey, M. G.; Hockless, D. C. R.; Skelton, B. W.; White, A. L. H. *Organometallics* **1995**, *14*, 3970. (h) Naulty, R. H.; McDonagh, A. M.; Whittall, I. R.; Cifuentes, M. P.; Humphrey, M. G.; Houbrechts, S.; Maes, J.; Persoons, A.; Schmid, S.; Hockless, D. C. R. *J. Organomet. Chem.* **1998**, *563*, 137.

(8) $[\text{Ni}(\eta^5\text{-C}_5\text{H}_5)(\text{PPh}_3)]$: Whittall, I. R.; Cifuentes, M. P.; Humphrey, M. G.; Luther-Davies, B.; Samoc, M.; Houbrechts, S.; Persoons, A.; Heath, G. A.; Bogsányi, D. *Organometallics* **1997**, *16*, 2631.

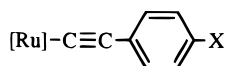
(9) $[\text{Au}(\text{PPh}_3)]$: Whittall, I. R.; Humphrey, M. G.; Houbrechts, S.; Persoons, A.; Hockless, D. C. R. *Organometallics* **1996**, *15*, 5738. See also refs 7b and 7f.

(10) (a) Cadierno, V.; Gamasa, M. P.; Gimeno, J.; Lastra, E.; Borge, J.; García-Granda, S. *Organometallics* **1994**, *13*, 745. (b) Cadierno, V.; Gamasa, M. P.; Gimeno, J.; Lastra, E. *J. Organomet. Chem.* **1994**, *474*, C27. (c) Cadierno, V.; Gamasa, M. P.; Gimeno, J.; Borge, J.; García-Granda, S. *J. Chem. Soc., Chem. Commun.* **1994**, 2495. (d) Cadierno, V.; Gamasa, M. P.; Gimeno, J.; González-Cueva, M.; Lastra, E.; Borge, J.; García-Granda, S. *Organometallics* **1996**, *15*, 2137. (e) Cadierno, V.; Gamasa, M. P.; Gimeno, J.; Borge, J.; García-Granda, S. *Organometallics* **1997**, *16*, 3178. (f) Cadierno, V.; Gamasa, M. P.; Gimeno, J.; López-González, M. C.; Borge, J.; García-Granda, S. *Organometallics* **1997**, *16*, 4453. (g) Cadierno, V.; Gamasa, M. P.; Gimeno, J.; Moretó, J. M.; Ricart, S.; Roig, A.; Molins, E. *Organometallics* **1998**, *17*, 697.

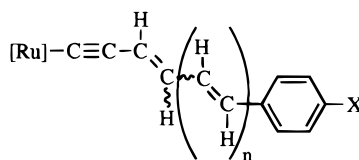
(11) (a) Houbrechts, S.; Clays, K.; Persoons, A.; Cadierno, V.; Gamasa, M. P.; Gimeno, J.; Whittall, I. R.; Humphrey, M. G. *Proc. SPIE-Int. Soc. Opt. Eng.* **1996**, *2852*, 98. (b) Houbrechts, S.; Clays, K.; Persoons, A.; Cadierno, V.; Gamasa, M. P.; Gimeno, J. *Organometallics* **1996**, *15*, 5266.

Chart 1

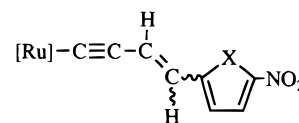
Complexes (A)



X = NO₂, C≡C-C₆H₄NO₂-4, N=CH-C₆H₄NO₂-4

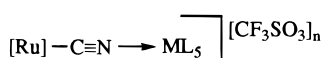


X = NO₂; n = 0, 1
X = CN; n = 0



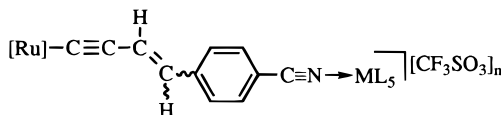
X = O, S

Complexes (B)



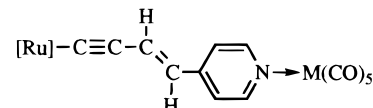
ML₅ = Cr(CO)₅, W(CO)₅; n = 0

ML₅ = Ru(NH₃)₅; n = 3



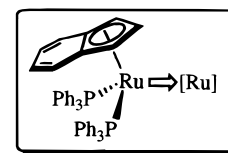
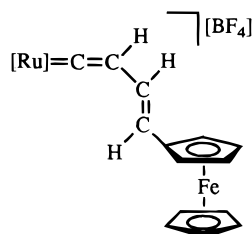
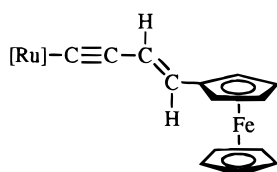
ML₅ = Cr(CO)₅, W(CO)₅; n = 0

ML₅ = Ru(NH₃)₅; n = 3

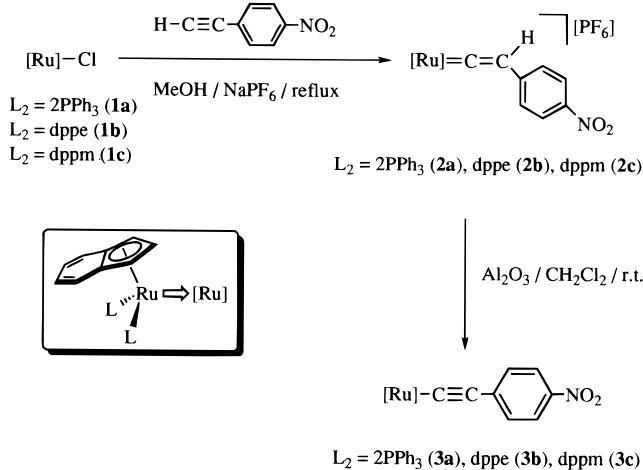


M = Cr, W

Complexes (C)



Scheme 1



isolated as air-stable hexafluorophosphate salts (49–67% yield) (Scheme 1). Spectroscopic data (IR and ¹H, ³¹P{¹H}, and ¹³C{¹H} NMR) clearly reveal the presence of the vinylidene moiety and can be compared with those reported for other indenylruthenium(II) vinylidene complexes (details are given in the Experimental Section).^{10,12} The most remarkable features of the NMR spectra are (i) (¹H NMR) the triplet (⁴J_{HP} = 1.5 Hz, **2a**)

or singlet (**2b,c**) resonance at δ 4.38–5.34 ppm of the Ru=C=CH proton and (ii) (¹³C NMR) the typical low-field resonance of the carbenic C_α, which appears as a triplet at δ 348.85–352.42 ppm (²J_{CP} = 14.7–16.5 Hz).

Compounds **2a–c** can be readily deprotonated by treatment with an excess of Al₂O₃ in dichloromethane, at room temperature, to give the donor–acceptor σ -alkynyl derivatives [Ru(C≡C–C₆H₄NO₂-4)(η^5 -C₉H₇)L₂] (**3a–c**) (42–79% yield) (Scheme 1).¹³ Complexes **3a–c** were analytically and spectroscopically characterized (see Tables 1 and 2 and Experimental Section). In particular, IR spectra exhibit the expected $\nu(\text{C}\equiv\text{C})$ absorption band in the range 2051–2060 cm⁻¹, and the ¹³C{¹H} NMR spectra show the C_α resonance which appears as a characteristic triplet signal at δ 136.44 ppm (²J_{CP} = 22.0 Hz) for complex **3c** and falls within the aromatic region (δ 127.39–141.97 ppm) for complexes **3a,b**. Comparison of these chemical shifts with that of the analogous complex [Ru(C≡C–C₆H₅)(η^5 -C₉H₇)(PPh₃)₂]^{12a} (δ 114.25 ppm) reveals a significant shift of the resonance to a lower field owing to the presence of the strong electron-withdrawing NO₂ group. The C_β resonance appears in all of the cases as a singlet in the range δ 115.13–117.77 ppm.

Treatment of [RuCl(η^5 -C₉H₇)(PPh₃)₂] (**1a**) with HC≡C–C₆H₄R-4 (R = C≡C–C₆H₄NO₂-4, N=CH–C₆H₄NO₂-4) and NaPF₆ in refluxing methanol also generates indenylruthenium(II) vinylidene complexes which were

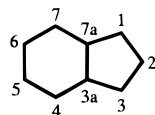
(12) (a) Gamasa, M. P.; Gimeno, J.; Martín-Vaca, B. M.; Borge, J.; García-Granda, S.; Pérez-Carreño, E. *Organometallics* **1994**, *13*, 4045. (b) Gamasa, M. P.; Gimeno, J.; Godefroy, I.; Lastra, E.; Martín-Vaca, B. M.; García-Granda, S.; Gutiérrez-Rodríguez, A. *J. Chem. Soc., Dalton Trans.* **1995**, 1901.

(13) The deprotonation of monosubstituted vinylidene complexes represents one of the most expeditious ways to achieve σ -alkynyl derivatives: Bruce, M. I. *Chem. Rev.* **1991**, *91*, 197.

Table 1. $^{31}\text{P}\{^1\text{H}\}$ and ^1H NMR Data for the Donor–Acceptor σ -Alkynyl Complexes^a

complex	$^{31}\text{P}\{^1\text{H}\}$	$\eta^5\text{-C}_9\text{H}_7^d$					others
		H-1,3	H-2	J_{HH}	H-4,7, H-5,6		
3a	51.50 s	4.73 d	5.53 t	2.2	6.25 m, 6.71 m		6.84–7.38 (m, PPh ₃ and C ₆ H ₂ H ₂ NO ₂ -4); 8.03 (d, C ₆ H ₂ H ₂ NO ₂ -4, $J_{\text{HH}} = 8.8$)
3b	86.65 s	5.01 d	5.11 t	2.5	<i>b, b</i>		1.82 and 2.25 (m, P(CH ₂) ₂ P); 6.49 and 7.80 (d, C ₆ H ₄ NO ₂ -4, $J_{\text{HH}} = 8.8$); 6.85–7.48 (m, PPh ₂)
3c	18.79 s	5.27 d	5.11 t	2.3	<i>b, b</i>		3.98 and 4.31 (m, PCH _a H _b P); 6.39 and 7.77 (d, C ₆ H ₄ NO ₂ -4, $J_{\text{HH}} = 8.7$); 6.92–7.45 (m, PPh ₂)
4	51.82 s	4.75 d	5.59 t	2.2	6.31 m, 6.70 m		6.87–7.68 (m, PPh ₃ and C ₆ H ₄ NO ₂ -4)
5	52.04 s	4.78 d	5.66 t	2.4	6.33 m, 6.71 m		6.84–7.84 (m, PPh ₃ and C ₆ H ₄ NO ₂ -4); 8.00 (s, =CH)
(E)-7a	51.60 s	4.74 d	5.63 t	2.0	6.28 m, 6.72 m		6.44 (d, =CH, $J_{\text{HH}} = 15.5$); 6.83–7.40 (m, PPh ₃ , =CH and C ₆ H ₂ H ₂ NO ₂ -4); 7.88 (d, C ₆ H ₂ H ₂ NO ₂ -4, $J_{\text{HH}} = 8.7$)
(Z)-7a	51.48 s	4.67 d	5.50 t	2.0	6.35 m, 6.74 m		6.06 and 6.47 (d, =CH, $J_{\text{HH}} = 11.2$); 6.83–7.40 (m, PPh ₃); 8.19 and 8.35 (d, C ₆ H ₄ NO ₂ -4, $J_{\text{HH}} = 8.8$)
(EE)-7b	51.44 s	4.74 d	5.66 t	2.2	<i>b, b</i>		6.12–7.61 (m, PPh ₃ , 4 =CH and C ₆ H ₂ H ₂ NO ₂ -4); 7.87 (d, C ₆ H ₂ H ₂ NO ₂ -4, $J_{\text{HH}} = 8.7$)
(ZE)-7b	52.01 s	4.68 d	5.45 t	2.2	<i>b, b</i>		6.12–7.61 (m, PPh ₃ , 4 =CH and C ₆ H ₂ H ₂ NO ₂ -4); 7.64 (d, C ₆ H ₂ H ₂ NO ₂ -4, $J_{\text{HH}} = 8.7$)
(E)-8a	51.41 s	4.70 d	5.56 t	2.4	6.25 m, <i>b</i>		5.43 (d, C ₄ H ₂ H ₂ NO ₂ -2,3, $J_{\text{HH}} = 3.7$); 6.15 (d, =CH, $J_{\text{HH}} = 15.4$); 6.25 (m, C ₄ H ₂ H ₂ NO ₂ -2,3); ^c 6.67–7.37 (m, PPh ₃ and =CH)
(Z)-8a	51.35 s	4.70 d	5.64 t	2.5	6.33 m, <i>b</i>		6.02 (d, =CH, $J_{\text{HH}} = 11.0$); 6.67–7.37 (m, PPh ₃ and =CH); 7.06 and 7.58 (d, C ₄ H ₂ ONO ₂ -2,3, $J_{\text{HH}} = 3.8$)
(E)-8b	49.87 s	5.00 d	6.23 t	2.4	6.16 m, 6.68 m		6.21 (d, =CH, $J_{\text{HH}} = 15.3$); 6.32 and 7.65 (d, C ₄ H ₂ SNO ₂ -2,3, $J_{\text{HH}} = 4.5$); 6.88–7.33 (m, PPh ₃ and =CH)
9	49.89 s	4.73 d	5.84 t	2.2	6.01 m, <i>b</i>		6.52 (s, =CH); 6.63–7.24 (m, PPh ₃ and 3H of C ₆ H ₄ NO ₂ -3); 7.59 (d, C ₆ H ₃ NO ₂ -3, $J_{\text{HH}} = 7.7$); 7.74 (dd, C ₆ H ₃ NO ₂ -3, $J_{\text{HH}} = 8.1$, $J_{\text{HH}} = 1.3$); 7.96 (dd, C ₆ H ₃ NO ₂ -3, $J_{\text{HH}} = 8.2$, $J_{\text{HH}} = 1.4$); 8.19 and 9.55 (s, C ₆ H ₃ NO ₂ -3)
(E)-13	51.66 s	4.73 d	5.63 t	2.2	6.30 m, 6.71 m		6.42 (d, =CH, $J_{\text{HH}} = 15.6$); 6.76–7.45 (m, PPh ₃ , =CH and C ₆ H ₄ CN-4)
(Z)-13	51.48 s	4.68 d	5.54 t	2.3	6.33 m, 6.71 m		6.03 (d, =CH, $J_{\text{HH}} = 11.4$); 6.76–7.45 (m, PPh ₃ , =CH and C ₆ H ₂ H ₂ CN-4); 8.32 (d, C ₆ H ₂ H ₂ CN-4, $J_{\text{HH}} = 8.4$)
(E)-14a	51.36 s	4.73 d	5.59 t	2.0	6.32 m, 6.72 m		6.42 (d, =CH, $J_{\text{HH}} = 15.8$); 6.83–7.54 (m, PPh ₃ , =CH and C ₆ H ₄ CN-4)
(Z)-14a	50.75 s	4.68 d	5.61 t	1.6	6.32 m, 6.72 m		6.32 (m, =CH); ^c 6.56 (d, C ₆ H ₂ H ₂ CN-4, $J_{\text{HH}} = 8.4$); 6.83–7.54 (m, PPh ₃ , =CH and C ₆ H ₂ H ₂ CN-4)
(E)-14b	51.37 s	4.73 d	5.60 t	2.0	6.30 m, 6.69 m		6.39 (d, =CH, $J_{\text{HH}} = 15.6$); 6.48 (d, C ₆ H ₂ H ₂ CN-4, $J_{\text{HH}} = 8.2$); 6.78–7.38 (m, PPh ₃ , =CH and C ₆ H ₂ H ₂ CN-4)
(Z)-14b	50.71 s	4.69 d	5.58 t	2.0	6.30 m, 6.69 m		5.99 (d, =CH, $J_{\text{HH}} = 11.1$); 6.78–7.38 (m, PPh ₃ , =CH and C ₆ H ₂ H ₂ CN-4); 8.23 (d, C ₆ H ₂ H ₂ CN-4, $J_{\text{HH}} = 8.5$)
(E)-16	51.40 s	4.74 d	5.66 t	2.2	6.29 m, 6.70 m		6.43 (d, =CH, $J_{\text{HH}} = 15.6$); 6.89–7.45 (m, PPh ₃ , =CH and C ₅ H ₂ H ₂ N-4); 8.51 (d, C ₅ H ₂ H ₂ N-4, $J_{\text{HH}} = 5.9$)
(E)-17a	51.92 s	4.73 d	5.62 t	2.2	6.25 m, 6.79 m		6.06 and 6.80 (d, =CH, $J_{\text{HH}} = 15.4$); 6.25 (m, C ₅ H ₂ H ₂ N-4); ^c 6.87–7.83 (m, PPh ₃ and C ₅ H ₂ H ₂ N-4)
(E)-17b	51.02 s	4.74 d	5.65 t	2.1	6.21 m, 6.70 m		6.05 (d, =CH, $J_{\text{HH}} = 15.4$); 6.17 and 7.86 (d, C ₅ H ₄ N-4, $J_{\text{HH}} = 6.5$); 6.79–7.35 (m, PPh ₃ and =CH)
(E)-18	51.69 s	4.73 d	5.70 t	2.2	6.30 m, 6.68 m		4.06 (s, C ₅ H ₅); 4.07 and 4.33 (m, C ₅ H ₄); 6.45 (d, =CH, $J_{\text{HH}} = 15.7$); 6.59 (dt, =CH, $J_{\text{HH}} = 15.7$, $J_{\text{HH}} = 1.6$); 6.94–7.50 (m, PPh ₃)

^a Spectra recorded in C₆D₆; δ in ppm and J in Hz. Abbreviations: s, singlet; d, doublet; dd, doublet of doublets; t, triplet; dt, doublet of triplets; m, multiplet. ^b Overlapped by PPh₃ or PPh₂ protons. ^c Overlapped by H-4,7 or H-5,6 protons. ^d Legend for indenyl skeleton.



not isolated but, instead, deprotonated in situ using an excess of Al₂O₃ (**4**) or K₂CO₃ (**5**) to afford the σ -alkynyl derivatives [Ru(C≡C–C₆H₄R-4)(η^5 -C₉H₇)(PPh₃)₂] (**4-5**) in 51% and 60% yield, respectively (Scheme 2). Complexes **4** and **5** display similar spectroscopic properties to those of complexes **3a–c** (see Tables 1 and 2 and Experimental Section).

σ -Enynyl Donor–Acceptor Complexes [Ru{C≡CCH=CR¹ (CH=CH)_nR²}(η^5 -C₉H₇)(PPh₃)₂] ($n = 0$, R¹ = H, R² = C₆H₄NO₂-4 [(*E*), (*Z*)-7a**], C₄H₂ONO₂-2,3 [(*E*), (*Z*)-**8a**], C₄H₂SNO₂-2,3 [(*E*)-**8b**]; $n = 0$, R¹ = R² = C₆H₄NO₂-3 (**9**); $n = 1$, R¹ = H, R² = C₆H₄NO₂-4 [(*EE*), (*ZE*)-**7b**]].** As is well-known, Wittig type reactions are one of the most useful procedures for the generation of double carbon–carbon bonds in organic synthesis.¹⁴ We have previously reported that alkynyl–phosphonio complexes [Ru{C≡CCH(R¹)(PR₃)}(η^5 -C₉H₇)(PPh₃)₂][PF₆]

(R¹ = H, Ph), containing an acidic hydrogen atom at C₇, are excellent substrates for Wittig reactions, leading to the formation of new double carbon–carbon bonds, i.e., [Ru(C≡CCR¹=CR²R³)(η^5 -C₉H₇)(PPh₃)₂].^{10c,g} Given the electron richness of the indenylruthenium(II) fragment, we believed that it would be of interest to exploit this methodology for the construction of novel σ -enynyl complexes with donor–acceptor properties of interest as materials with good NLO properties. Therefore, we set up a series of Wittig reactions using unsaturated aldehydes and ketones bearing the NO₂ acceptor group. The formation of the new double carbon–carbon bond should give rise to the generation of a π -conjugated system of a triple and double carbon–carbon bonds

(14) For example, see: Kelly, S. E. In *Comprehensive Organic Synthesis*; Trost, B. M., Fleming, I., Eds.; Pergamon: Oxford, 1991; Vol. 1, p 755.

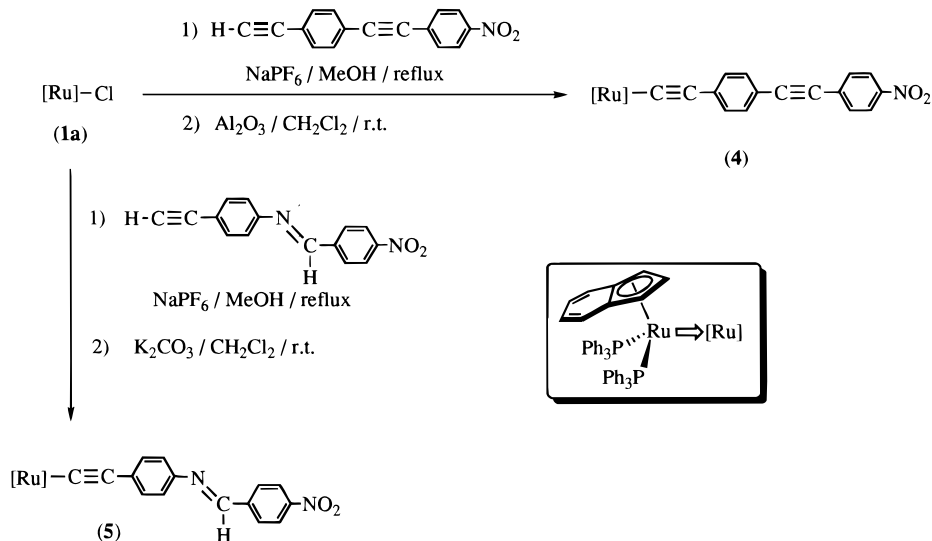
Table 2. $^{13}\text{C}\{^1\text{H}\}$ NMR Data for the Donor–Acceptor σ -Alkynyl Complexes^a

complex	$\eta^5\text{-C}_9\text{H}_7$					Ru–C $_{\alpha}$	$^2J_{\text{CP}}$	C $_{\beta}$	others
	C-1,3	C-2	C-3a,7a	$\Delta\delta(\text{C-3a,7a})^b$	C-4,7, C-5,6				
3a	76.05	95.93	110.23	–20.47	<i>c, c</i>	<i>d</i>	<i>d</i>	117.77	127.39–129.64 (m, PPh ₃ , CH of C ₆ H ₄ NO ₂ -4 and C of C ₆ H ₄ NO ₂ -4); 131.30 (s, C of C ₆ H ₄ NO ₂ -4)
3b	71.12	93.50	108.69	–22.01	<i>d, d</i>	<i>d</i>	<i>d</i>	115.13	28.84 (m, P(CH ₂) ₂ P); 124.08–141.97 (m, PPh ₂ and CH of C ₆ H ₄ NO ₂ -4); 138.12 and 144.03 (s, C of C ₆ H ₄ NO ₂ -4)
3c	68.42	89.96	107.33	–23.37	<i>d, d</i>	136.44 t	22.0	115.18	50.30 (t, PCH ₂ P, $J_{\text{CP}} = 23.4$); 123.27–138.54 (m, PPh ₂ and CH of C ₆ H ₄ NO ₂ -4); 137.41 and 143.36 (s, C of 4 C ₆ H ₄ NO ₂ -4)
4	75.10	94.86	109.16	–21.54	<i>d, d</i>	125.20 t	24.4	<i>e</i>	88.39 and 96.73 (s, =C); 123.19–138.62 (m, PPh ₃ , CH of C ₆ H ₄ and C ₆ H ₄ NO ₂ -4, and C of C ₆ H ₄ or C ₆ H ₄ NO ₂ -4); 146.93 (s, C of C ₆ H ₄ or C ₆ H ₄ NO ₂ -4)
5	75.12	95.49	109.51	–21.19	<i>f, f</i>	118.63 t	24.8	115.67	127.50–138.99 (m, PPh ₃); 131.00, 142.18, 146.38 and 148.97 (s, C of C ₆ H ₄ and C ₆ H ₄ NO ₂ -4); 154.13 (s, =CH)
(E)–7a	75.96	96.06	110.41	–20.29	<i>d, d</i>	133.66 t	24.5	118.36	121.43 (s, =CH); 123.85–139.58 (m, PPh ₃ , =CH and CH of C ₆ H ₄ NO ₂ -4); 146.34 and 146.71 (s, C of C ₆ H ₄ NO ₂ -4)
(Z)–7a	75.58	95.81	110.60	–20.10	<i>d, d</i>	141.39 t	23.9	119.04	120.48 (s, =CH); 123.85–139.58 (m, PPh ₃ , =CH and CH of C ₆ H ₄ NO ₂ -4); 146.27 and 146.41 (s, C of C ₆ H ₄ NO ₂ -4)
(EE)–7b	75.25	95.49	109.79	–20.91	<i>d, d</i>	<i>d</i>	<i>d</i>	118.50	125.05, 132.69 and 136.40 (s, =CH); 123.22–138.82 (m, PPh ₃ , =CH and CH of C ₆ H ₄ NO ₂ -4); 145.05 and 145.93 (s, C of C ₆ H ₄ NO ₂ -4)
(ZE)–7b	75.05	95.36	109.72	–20.98	<i>d, d</i>	132.47 t	25.1	116.71	120.94, 131.41, and 133.71 (s, =CH); 123.22–138.82 (m, PPh ₃ , =CH and CH of C ₆ H ₄ NO ₂ -4); 145.11 and 145.88 (s, C of C ₆ H ₄ NO ₂ -4)
(E)–8a	76.11	96.07	110.45	–20.25	123.84, 127.03	140.86 t	24.3	119.19	107.45, 110.74 and 115.25 (s, CH of C ₄ H ₂ ONO ₂ -2,3 and =CH); 127.38–139.12 (m, PPh ₃ and CH of C ₄ H ₂ ONO ₂ -2,3 or =CH); 159.28 and 159.38 (s, C of C ₄ H ₂ ONO ₂ -2,3)
(Z)–8a	75.83	95.88	110.45	–20.25	124.05, 127.17	147.08 t	24.3	119.77	108.09, 121.44 and 122.70 (s, CH of C ₄ H ₂ ONO ₂ -2,3 and =CH); 127.38–139.12 (m, PPh ₃ and CH of C ₄ H ₂ ONO ₂ -2,3 or =CH); 150.75 and 151.77 (s, C of C ₄ H ₂ ONO ₂ -2,3)
(E)–8b	76.25	96.39	111.04	–19.66	124.20, 127.10	<i>d</i>	<i>d</i>	<i>d</i>	120.10, 122.13, 124.84, and 129.34 (s, CH of C ₄ H ₂ SNO ₂ -2,3 and =CH); 128.21–139.01 (m, PPh ₃); 145.71 and 152.87 (s, C of C ₄ H ₂ SNO ₂ -2,3)
9	75.26	95.47	110.07	–20.63	123.23, 126.09	<i>d</i>	<i>d</i>	116.07	119.83, 121.08, 121.66, 122.30 and 125.36 (s, =CH and CH of C ₆ H ₄ NO ₂ -3); 127.48–138.64 (m, PPh ₃ and CH of C ₆ H ₄ NO ₂ -3); 142.27, 144.80, 148.81, and 148.98 (s, C of C ₆ H ₄ NO ₂ -3)
(E)–13	75.26	95.36	109.72	–20.98	<i>d, d</i>	129.31 t	24.7	<i>g</i>	108.90 (s, C≡N); 119.53 (s, =CH); 123.23–138.82 (m, PPh ₃ , =CH and CH of C ₆ H ₄ CN-4); 143.81 (s, C of C ₆ H ₄ CN-4)
(Z)–13	74.92	95.18	109.92	–20.78	<i>d, d</i>	137.19 t	22.3	<i>h</i>	109.14 (s, C≡N); 118.70 (s, =CH); 123.43–138.82 (m, PPh ₃ , =CH and CH of C ₆ H ₄ CN-4); 143.61 (s, C of C ₆ H ₄ CN-4)
(E)–14a	75.28	95.36	109.71	–20.99	<i>d, d</i>	<i>d</i>	<i>d</i>	<i>i</i>	108.80 (s, C≡N); 119.58 (s, =CH); 123.22–135.90 (m, PPh ₃ , =CH and CH of C ₆ H ₄ CN-4); 143.85 (s, C of C ₆ H ₄ CN-4); 214.71 and 219.67 (s, C≡O)
(Z)–14a	74.92	95.16	109.79	–20.91	<i>d, d</i>	<i>d</i>	<i>d</i>	<i>j</i>	105.80 (s, C≡N); 120.84 (s, =CH); 123.22–135.90 (m, PPh ₃ , =CH and CH of C ₆ H ₄ CN-4); 145.07 (s, C of C ₆ H ₄ CN-4); 214.71 and 219.67 (s, C≡O)
(E)–14b	75.36	95.37	109.79	–20.91	<i>d, d</i>	135.38 t	24.3	117.79	104.80 (s, C≡N); 109.70 and 145.49 (s, C of C ₆ H ₄ CN-4); 118.50–138.64 (m, PPh ₃ , =CH and CH of C ₆ H ₄ CN-4); 197.00 and 200.31 (s, C≡O)
(Z)–14b	75.05	95.11	109.98	–20.72	<i>d, d</i>	142.45 t	23.8	116.61	105.12 (s, C≡N); 108.77 and 145.08 (s, C of C ₆ H ₄ CN-4); 118.50–138.64 (m, PPh ₃ , =CH and CH of C ₆ H ₄ CN-4); 199.30 and 201.32 (s, C≡O)
(E)–16	75.86	96.05	110.34	–20.36	<i>k, k</i>	<i>d</i>	<i>d</i>	116.82	120.68 (s, =CH); 128.22–139.67 (m, PPh ₃ and =CH); 146.93 (s, C of C ₅ H ₄ N-4); 151.09 (s, CH of C ₅ H ₄ N-4)
(E)–17a	75.31	95.34	108.89	–21.81	<i>l, l</i>	138.51 t	24.4	117.88	126.66 (s, =CH); 127.28–138.61 (m, PPh ₃ and =CH); 147.65 (s, C of C ₅ H ₄ N-4); 154.74 (s, CH of C ₅ H ₄ N-4); 215.33 and 221.18 (s, C≡O)
(E)–17b	76.01	96.01	110.57	–20.13	<i>m, m</i>	141.67 t	24.5	119.11	127.83 (s, =CH); 128.23–139.43 (m, PPh ₃ and =CH); 148.39 (s, C of C ₅ H ₄ N-4); 155.90 (s, CH of C ₅ H ₄ N-4); 200.23 and 203.46 (s, C≡O)
(E)–18	74.87	95.60	109.55	–21.15	123.16, 125.95	113.97 t	24.8	115.01	66.16 and 68.52 (s, CH of C ₅ H ₄); 69.67 (s, C ₅ H ₅); 86.31 (s, C of C ₅ H ₄); 113.61 and 129.43 (s, =CH); 127.45–138.94 (m, PPh ₃)

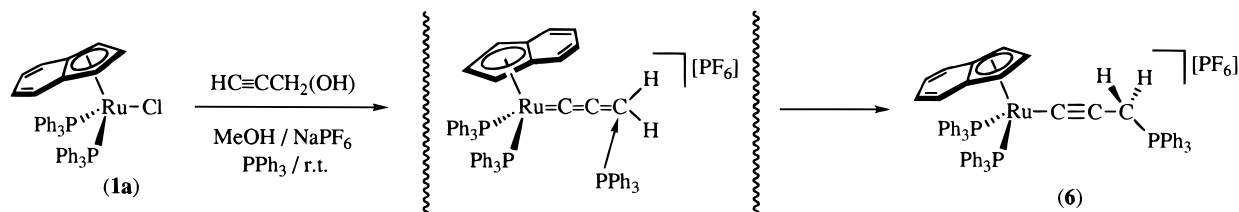
Table 2 (Continued)

^a Spectra recorded in C₆D₆; δ in ppm and J in Hz. Abbreviations: s, singlet; t, triplet; m, multiplet. ^b $\Delta\delta(\text{C-3a,7a}) = \delta(\text{C-3a,7a}(\eta^5\text{-indenyl complex})) - \delta(\text{C-3a,7a}(\text{sodium indenyl}))$, $\delta(\text{C-3a,7a})$ for sodium indenyl 130.70 ppm. See ref 17. ^c 123.84, 124.69 and 127.04 ppm (s, C-4,7, C-5,6 and CH of C₆H₄NO₂-4). ^d Overlapped by PPh₃ or PPh₂ carbons. ^e 115.67 and 115.92 ppm (s, C_β and C of C₆H₄ or C₆H₄NO₂-4). ^f 121.97, 123.21, 123.81, 126.14, 128.34 and 131.85 ppm (s, C-4,7, C-5,6 and CH of C₆H₄ and C₆H₄NO₂-4). ^g 116.64 and 119.68 ppm (s, C_β and C of C₆H₄CN-4). ^h 117.43 and 119.90 ppm (s, C_β and C of C₆H₄CN-4). ⁱ 116.65 and 119.72 ppm (s, C_β and C of C₆H₄CN-4). ^j 117.52 and 118.77 ppm (s, C_β and C of C₆H₄CN-4). ^k 120.12, 123.83 and 126.89 ppm (s, C-4,7, C-5,6 and CH of C₅H₄N-4). ^l 119.80, 123.20 and 126.42 ppm (s, C-4,7, C-5,6 and CH of C₅H₄N-4). ^m 120.82, 123.85 and 127.18 ppm (s, C-4,7, C-5,6 and CH of C₅H₄N-4).

Scheme 2



Scheme 3

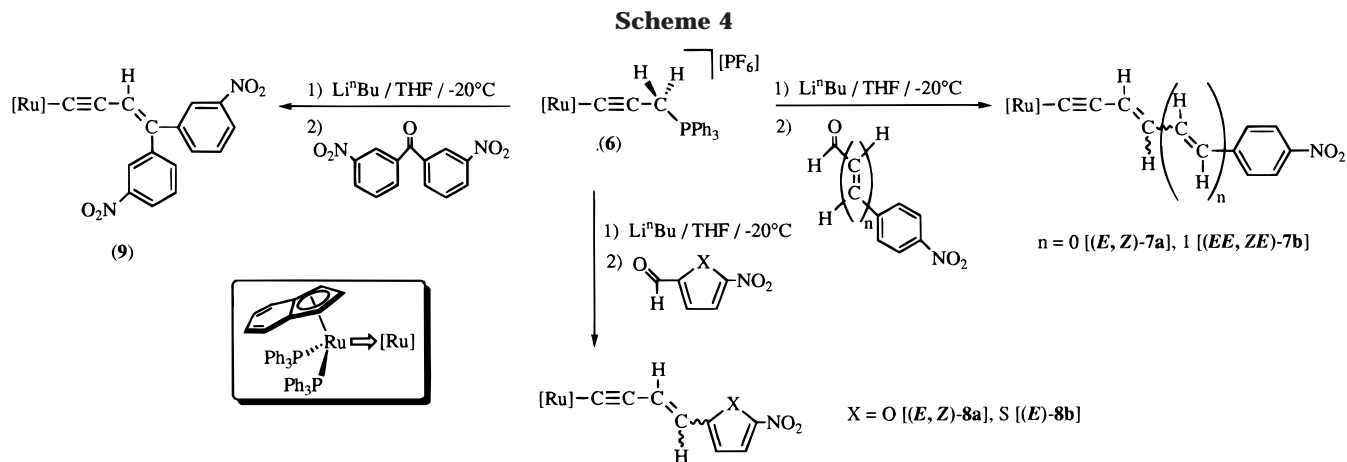


supporting the acceptor group at the end of the unsaturated chain. The starting material for the Wittig type reactions is the alkynyl–phosphonio derivative $[\text{Ru}\{\text{C}\equiv\text{CCH}_2(\text{PPh}_3)\}(\eta^5\text{-C}_9\text{H}_7)(\text{PPh}_3)_2][\text{PF}_6]$ (**6**) which is obtained in a one-pot synthesis by treatment of complex **1a** with 2-propyn-1-ol and NaPF₆ in methanol, at room temperature, and in the presence of a large excess of triphenylphosphine (65% yield) (Scheme 3).^{15a} Analytical and spectroscopic data are in accordance with this formulation (see Experimental Section).^{10b,e,f}

(15) (a) We have recently reported that alkynyl–phosphonio complexes can be readily prepared through the regioselective nucleophilic addition of phosphines to the C₇ atom of indenylruthenium(II) allenylidene complexes $[\text{Ru}(\text{C}=\text{C}=\text{CR}_2)(\eta^5\text{-C}_9\text{H}_7)\text{L}_2][\text{PF}_6]$ (see refs 10b,e,f). Thus, the formation of **6** may be understood assuming that the unsubstituted allenylidene intermediate $[\text{Ru}(\text{C}=\text{C}=\text{CH}_2)(\eta^5\text{-C}_9\text{H}_7)(\text{PPh}_3)_2][\text{PF}_6]$ is formed as a transient species which undergoes a rapid nucleophilic addition of triphenylphosphine to the electrophilic C₇ atom. (b) Due to the relative imprecision of the crystallographic determination some caution must be considered in the reliable interpretation of these data. (c) This fact contrasts with the values of the bond lengths found in similar systems, i.e., $[\text{Ru}(\text{E})\text{-4,4}'\text{-C}\equiv\text{C}-\text{C}_6\text{H}_4-\text{CH}=\text{CH}-\text{C}_6\text{H}_4-\text{NO}_2](\eta^5\text{-C}_5\text{H}_5)(\text{PPh}_3)_2$ ^{7a} and $[\text{Ru}(\text{E})\text{-4,4}'\text{-C}\equiv\text{C}-\text{C}_6\text{H}_4-\text{C}\equiv\text{C}-\text{C}_6\text{H}_4-\text{NO}_2](\eta^5\text{-C}_5\text{H}_5)(\text{PPh}_3)_2$ ^{7d} which are consistent with the sequence of single, double, and single bond (–CH=CH–) or single, triple, and single bond (–C≡C–), respectively. (d) Iglesias, L. Ph.D. Thesis, University of Oviedo, 1998. Preliminary theoretical studies using ab initio calculations (Gaussian94) establish that a molecular minimum energy value is achieved by the π overlapping of the metal fragment LUMO with the corresponding π orbital of the 4-nitroarylenynyl chain, as shown in Figure 3.

The treatment of a yellow THF solution of complex **6** with 1 equiv of LiⁿBu at –20 °C gives rise to an immediate change to a violet solution probably containing the iylde–alkynyl derivative $[\text{Ru}(\text{C}\equiv\text{CCH}=\text{PPh}_3)(\eta^5\text{-C}_9\text{H}_7)(\text{PPh}_3)_2]$. Subsequent addition of nitro-substituted unsaturated aldehydes, after the mixture was allowed to reach room temperature, results in the formation of σ -enynyl complexes **7–8a,b** (41–90% yield) (Scheme 4).

Complex **8b** was isolated as the *E* stereoisomer while complexes **7a,b** and **8a** were obtained as an unseparable mixture of the *E* and *Z* stereoisomers (2/1, 4/3, and 3/2, respectively). All attempts to form these compounds stereoselectively were unsuccessful. Similarly, the σ -enynyl complex **9** was obtained (88% yield) from the reaction of **6** with LiⁿBu and 3,3'-dinitrobenzophenone. The spectroscopic properties (see Tables 1 and 2 and Experimental Section) of all of these complexes are consistent with the proposed formulations. Significant features are (a) the $\nu(\text{C}\equiv\text{C})$ IR absorption band (2021–2041 cm^{–1}), (b) the typical triplet resonance in the ¹³C{¹H} NMR spectra for the Ru–C≡ carbon nucleus at δ 123.85–147.08 ppm (²J_{CP} = 23.9–25.1 Hz), (c) singlet signals of C_β and the olefinic carbons in the range ca. δ 110–140 ppm (assigned using DEPT experiments) (see Table 2), and (d) the olefinic protons resonances, in the ¹H NMR spectra, which appear at ca. δ 6–7 ppm (see Table 1).



Similar to the complexes **3a–c**, the chemical shifts of the α carbon atom attached to ruthenium are sensitive to the electronic delocalization through the enynyl chain as expected by the presence of the strong electron attractor NO_2 group at the end of the chain. Thus, if the C_α resonance in complex $[\text{Ru}(\text{C}\equiv\text{C}-\text{C}_6\text{H}_5)(\eta^5-\text{C}_9\text{H}_7)(\text{PPh}_3)_2]$ (δ 114.25 ppm)^{12a} is compared with those of complexes **3a**, **7a**, and **7b** (δ ca. 128, 141.39 (*Z*) and 132.47 (*ZE*) ppm, respectively), a downfield shifting of ca. 13–27 ppm occurs. It is interesting to note that the assembling of a second $\text{CH}=\text{CH}$ moiety in the dienynyl complex **7b** with respect to the enynyl **7a** hardly affects the electronic delocalization. As it will be discussed below, this is in accord with the NLO properties. In a lesser extent a similar downfield shifting (4–5 ppm) is observed for the C_β resonance.

To confirm the connectivity and to obtain information on the potential electronic π -conjugation in the unsaturated hydrocarbon chains, the structure of complexes **7b** and **9** have been determined by X-ray crystallography.

X-ray Crystal Structures of $[\text{Ru}\{\text{C}\equiv\text{C}-(\text{CH}=\text{CH})_2-\text{C}_6\text{H}_4\text{NO}_2\}\{\eta^5-\text{C}_9\text{H}_7\}(\text{PPh}_3)_2]$ (7b**) and $[\text{Ru}\{\text{C}\equiv\text{C}-\text{CH}=\text{C}(\text{C}_6\text{H}_4\text{NO}_2)_2\}\{\eta^5-\text{C}_9\text{H}_7\}(\text{PPh}_3)_2]$ (**9**).** Both crystal structures consist of molecules of the complex together with solvent molecules of crystallization (pentane–THF and 2THF for **7b** and **9**, respectively). Moreover, crystals only of the *EE* stereoisomer of the complex (*EE, ZE*)-**7b** were obtained by slow diffusion of pentane in a solution of the complex in THF. ORTEP views of the molecular geometries of **7b** and **9** are shown in Figures 1 and 2. Selected bond distances and angles are listed in Table 3. Both molecules exhibit the usual pseudooctahedral three-legged piano stool geometry with the η^5 -indenyl ligand in the usual allylene coordination mode. The interligand angles $\text{P}(1)-\text{Ru}-\text{P}(2)$, $\text{C}(1)-\text{Ru}-\text{P}(1)$, and $\text{C}(1)-\text{Ru}-\text{P}(2)$, and those between the centroid C^* and the legs show values typical of a pseudooctahedron (see Table 3). $\text{Ru}-\text{P}$ bond distances of 2.300(8)–2.327(3) Å are in the range of other ruthenium(II) indenyl complexes,^{10,12} but the Ru–

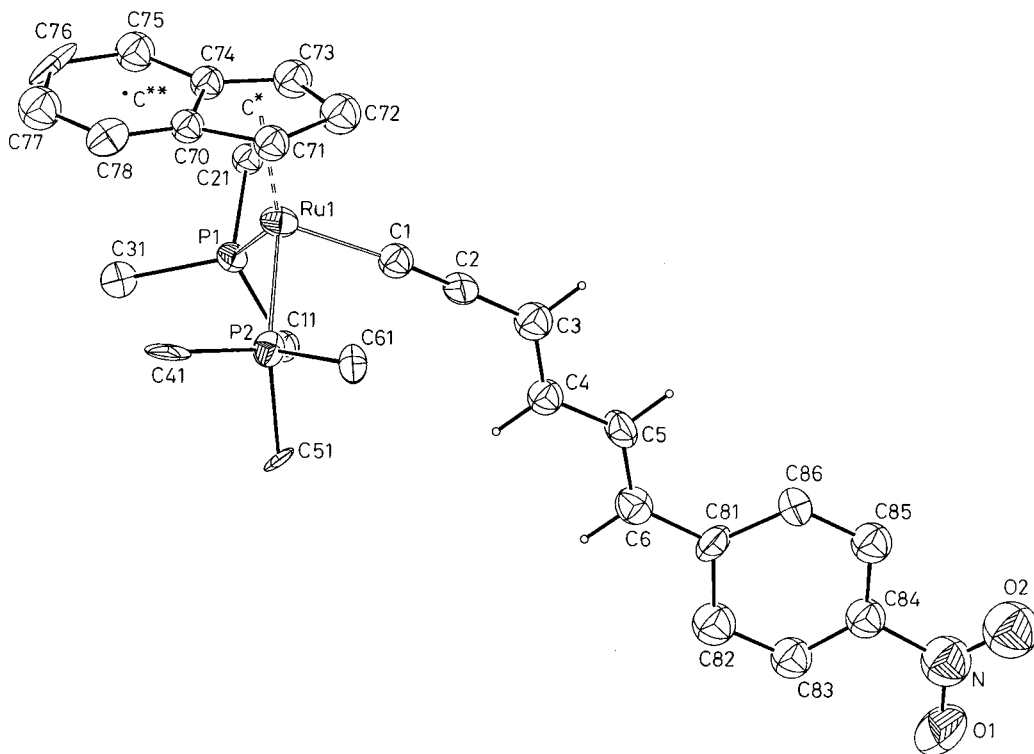


Figure 1. ORTEP view of the structure of $(EE)\text{-}[\text{Ru}\{\text{C}\equiv\text{C}(\text{CH}=\text{CH})_2-\text{C}_6\text{H}_4\text{NO}_2\}\{\eta^5-\text{C}_9\text{H}_7\}(\text{PPh}_3)_2]$ [(*EE*)-**7b**]. For clarity, aryl groups of the triphenylphosphine ligands are omitted (C^* = centroid of the indenyl ring).

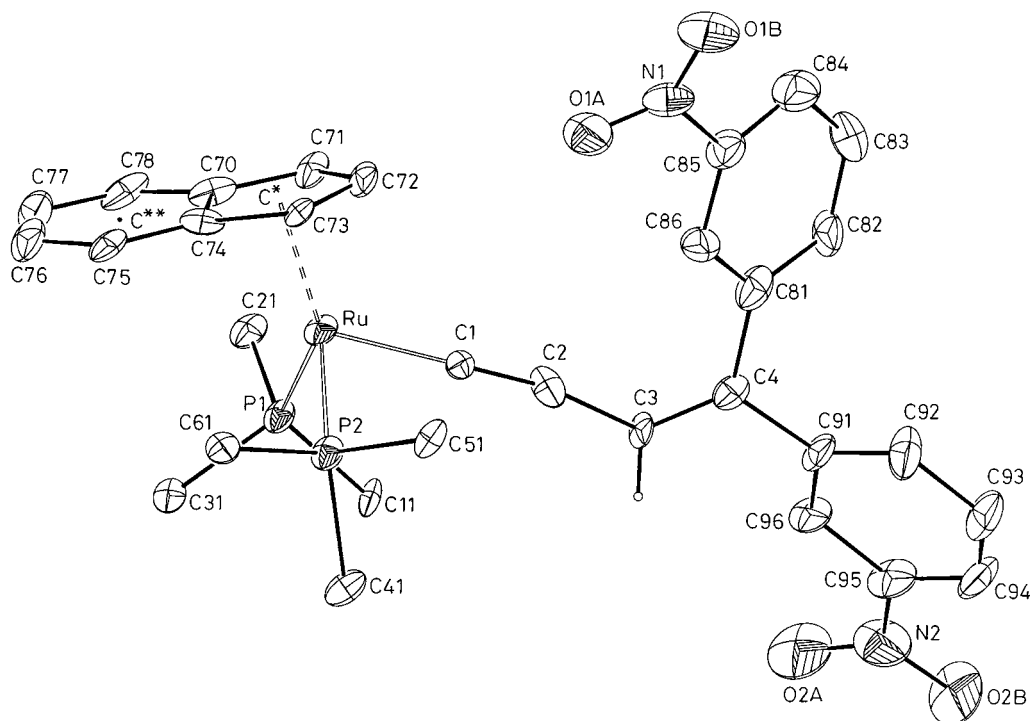


Figure 2. ORTEP view of the structure of $[\text{Ru}\{\text{C}\equiv\text{CCH}=\text{C}(\text{C}_6\text{H}_4\text{NO}_2\text{-}3)\}_2](\eta^5\text{-C}_9\text{H}_7)(\text{PPh}_3)_2$ (**9**). For clarity, aryl groups of the triphenylphosphine ligands are omitted (C^* = centroid of the indenyl ring).

$\text{C}(1)$ bond length values for **7b** and **9** of 1.99(2) and 1.97(1) Å, respectively, are among the shortest ones reported for alkynyl complexes.^{7d,g} The enynyl groups are almost linearly attached to ruthenium with angles $\text{Ru}-\text{C}(1)-\text{C}(2)$ of 172.2(2)° (**7b**) and 179.6(9)° (**9**) and $\text{C}(1)-\text{C}(2)-\text{C}(3)$ of 178.3(3)° (**7b**) and 169.1(1)° (**9**). Complex **7b** contains the first structurally characterized example of a dienyl-acetylide chain bonded to a metal fragment. Within the unsaturated seven carbon chain $\text{C}(1)-\text{C}(2)-\text{C}(3)-\text{C}(4)-\text{C}(5)-\text{C}(6)-\text{C}(81)$ the $\text{C}-\text{C}$ separations are 1.19(3), 1.38(3), 1.35(2), 1.35(3), 1.34(3), and 1.44(3) Å, respectively. It is worth noting the similar and relatively short $\text{C}-\text{C}$ distances (1.35(2) Å av) observed in that part of the chain involving the sequence of single and double bonds i.e. the $\text{C}(2)-\text{C}(6)$ fragment.^{15b} In contrast, the $\text{C}-\text{C}$ distances of the enynyl chain $\text{C}(1)-\text{C}(4)$ in complex **9** are consistent with a typical sequence of triple, single, and double bonds, i.e., 1.23(1), 1.42(2), and 1.31(1) Å, respectively. Although apparently there is no contribution of a potential quinoidal resonant form (distances and angles of the nitro substituents and aryl group in both complexes **9** and **7b** are unexceptional), the absence of bond length alternation of the $\text{C}-\text{C}$ distances in $\text{C}(2)-\text{C}(6)$ seems to indicate that there is an extensive electronic delocalization.^{15c} In accordance with this fact, the structure of **7b** shows that all of the atoms of the dienynyl chain and those of the nitroaryl ring are approximately in a plane as is shown in Figure 3. The deviations of the atoms from the mean least-squares plane passing through them being in the range of $\text{N} -0.0808$ to $\text{C}(3) -0.2515$ Å (Table 3). Another interesting feature of this structure is the small dihedral angle of 7.6(9)° between the mean plane containing the hydrocarbon chain and the pseudo mirror plane of the metallic moiety (containing the Ru atom, the $\text{C}(1)$ atom, and the centroid C^* of the five carbon ring of the indenyl ligand). Although we have not studied the features of

the bonding between the metal fragment and the enynyl group this particular orientation seems to favor the maximum overlapping of the metallic π frontier orbital with the π system of the conjugated dienynyl group.^{15d} This is in accordance with the good NLO properties shown by complex **7b** which probably stems from the good electronic communication between the donor metal fragment and the strong acceptor nitroaryl group through the hydrocarbon chain (see below).

Bimetallic Donor–Acceptor Complexes $[(\eta^5\text{-C}_9\text{H}_7)(\text{PPh}_3)_2\text{Ru}\{\mu\text{-C}\equiv\text{N}\}\text{ML}_5][\text{CF}_3\text{SO}_3]_n$ ($n = 0$, $\text{ML}_5 = \text{Cr}(\text{CO})_5$ (**11a**), $\text{W}(\text{CO})_5$ (**11b**); $n = 3$, $\text{ML}_5 = \text{Ru}(\text{NH}_3)_5$ (**12**)), $[(\eta^5\text{-C}_9\text{H}_7)(\text{PPh}_3)_2\text{Ru}\{\mu\text{-C}\equiv\text{CCH}=\text{CH}-\text{C}_6\text{H}_4\text{C}\equiv\text{N}\}\text{ML}_5][\text{CF}_3\text{SO}_3]_n$ ($n = 0$, $\text{ML}_5 = \text{Cr}(\text{CO})_5$ [**(E,Z)-14a**], $\text{W}(\text{CO})_5$ [**(E,Z)-14b**]; $n = 3$, $\text{ML}_5 = \text{Ru}(\text{NH}_3)_5$ [**(E,Z)-15**]), and $[(\eta^5\text{-C}_9\text{H}_7)(\text{PPh}_3)_2\text{Ru}\{\mu\text{-C}\equiv\text{CCH}=\text{CH}-\text{C}_5\text{H}_4\text{N}\}\text{M}(\text{CO})_5]$ ($\text{M} = \text{Cr}$ [**(E)-17a**], W [**(E)-17b**]). An alternative entry to the donor–acceptor complexes is based on the synthesis of mixed valence dinuclear metallic species providing that a good electronic coupling between the donor and acceptor metallic moieties can be established. In this regard we sought to synthesize novel dinuclear derivatives by using the indenylruthenium(II) fragment $[\text{Ru}(\eta^5\text{-C}_9\text{H}_7)(\text{PPh}_3)_2]$ as the donor moiety attached to a formally acceptor metallic fragment through the coordination of an unsaturated bridging group. We were specially interested in studying the influence of the acceptor metallic moiety on the quadratic hyperpolarizabilities

(16) (a) Loucif-Saibi, R.; Delaire, J. A.; Bonazzola, L.; Doisneau, G.; Balavoine, G.; Fillebeen-Khan, T.; Ledoux, I.; Puccetti, G. *Chem. Phys.* **1992**, *167*, 369. (b) Laidlaw, W. M.; Denning, R. G.; Verbiest, T.; Chouchard, E.; Persoons, A. *Nature* **1993**, *363*, 58. (c) Behrens, U.; Brussaard, H.; Hagenau, U.; Heck, J.; Hendricks, E.; Kornich, J.; van der Linden, J. G. M.; Persoons, A.; Speck, A. L.; Veldman, N.; Voss, B.; Wong, H. *Chem. Eur. J.* **1996**, *2*, 98. (d) Mata, J.; Uriel, S.; Peris, E.; Llusar, R.; Houbrechts, S.; Persoons, A. *J. Organomet. Chem.* **1998**, *562*, 197.

Table 3. Selected Bond Distances and Slip Parameter $D^a(\text{Å})$ and Bond Angles and Dihedral Angles FA^b , HA^c , and $CA^d(\text{deg})$ for $[\text{Ru}\{\text{C}\equiv\text{C}-(\text{CH}=\text{CH})_2-\text{C}_6\text{H}_4\text{NO}_2-4\}(\eta^5-\text{C}_9\text{H}_7)(\text{PPh}_3)_2].\text{THF}/n\text{-C}_5\text{H}_{12}$ (7b**) and $[\text{Ru}\{\text{C}\equiv\text{C}-\text{CH}=\text{C}(\text{C}_6\text{H}_4\text{NO}_2-3)_2\}(\eta^5-\text{C}_9\text{H}_7)(\text{PPh}_3)_2].2\text{THF}$ (**9**)**

Complex 9							
Distances							
Ru-C*	1.94(1)	P(2)-C(51)	1.86(1)	C(1)-C(2)	1.23(1)	C(75)-C(76)	1.35(2)
Ru-C(1)	1.97(1)	P(2)-C(61)	1.84(1)	C(2)-C(3)	1.42(2)	C(76)-C(77)	1.40(2)
Ru-P(1)	2.327(3)	C(81)-C(82)	1.37(2)	C(3)-C(4)	1.31(1)	C(77)-C(78)	1.36(2)
Ru-P(2)	2.320(3)	C(82)-C(83)	1.37(2)	C(4)-C(81)	1.50(2)	C(91)-C(92)	1.37(2)
Ru-C(70)	2.39(1)	C(83)-C(84)	1.43(2)	C(4)-C(91)	1.48(2)	C(92)-C(93)	1.40(2)
Ru-C(71)	2.25(1)	C(84)-C(85)	1.36(2)	C(70)-C(78)	1.40(2)	C(93)-C(94)	1.36(2)
Ru-C(72)	2.18(1)	C(85)-C(86)	1.36(2)	C(70)-C(74)	1.49(1)	C(94)-C(95)	1.38(2)
Ru-C(73)	2.212(9)	C(86)-C(81)	1.42(2)	C(70)-C(71)	1.39(2)	C(95)-C(96)	1.42(2)
Ru-C(74)	2.37(1)	C(85)-N(1)	1.52(1)	C(71)-C(72)	1.42(2)	C(96)-C(91)	1.42(2)
P(1)-C(11)	1.84(1)	N(1)-O(1A)	1.21(1)	C(72)-C(73)	1.35(2)	C(95)-N(2)	1.48(2)
P(1)-C(21)	1.84(1)	N(1)-O(1B)	1.20(1)	C(73)-C(74)	1.41(2)	N(2)-O(2A)	1.24(2)
P(1)-C(31)	1.83(1)	Δ	0.15(1)	C(74)-C(75)	1.42(2)	N(2)-O(2B)	1.24(2)
P(2)-C(41)	1.87(1)						
Angles							
C*-Ru-P(1)	124.4(3)	C(86)-C(81)-C(4)	120.1	C(71)-C(70)-C(78)	137.1	C(92)-C(91)-C(4)	122.1
C*-Ru-P(2)	121.8(4)	C(83)-C(82)-C(81)	122.1	C(71)-C(70)-C(74)	107.1	C(96)-C(91)-C(4)	119.1
C*-Ru-C(1)	122.9(5)	C(82)-C(83)-C(84)	120.1	C(70)-C(71)-C(72)	108.1	C(93)-C(92)-C(91)	122.1
C(1)-Ru-P(1)	86.3(3)	C(85)-C(84)-C(83)	115.1	C(73)-C(72)-C(71)	109.1	C(92)-C(93)-C(94)	120.2
C(1)-Ru-P(2)	87.1(3)	C(84)-C(85)-C(86)	127.1	C(72)-C(73)-C(74)	111.1	C(95)-C(94)-C(93)	119.1
P(2)-Ru-P(1)	103.9(1)	C(84)-C(85)-N(1)	115.1	C(73)-C(74)-C(75)	136.1	C(94)-C(95)-C(96)	122.1
C(2)-C(1)-Ru	179.6(9)	C(86)-C(85)-N(1)	117.1	C(73)-C(74)-C(70)	104.1	C(94)-C(95)-N(2)	121.1
C(1)-C(2)-C(3)	169.1	C(85)-C(86)-C(81)	116.1	C(75)-C(74)-C(70)	120.1	C(96)-C(95)-N(2)	117.2
C(4)-C(3)-C(2)	130.1	O(1B)-N(1)-C(85)	117.1	C(76)-C(75)-C(74)	120.1	C(95)-C(96)-C(91)	117.1
C(3)-C(4)-C(81)	124.1	O(1B)-N(1)-O(1A)	126.1	C(75)-C(76)-C(77)	122.1	O(2B)-N(2)-O(2A)	124.2
C(3)-C(4)-C(91)	121.1	O(1A)-N(1)-C(85)	117.1	C(78)-C(77)-C(76)	121.1	O(2B)-N(2)-C(95)	116.2
C(91)-C(4)-C(81)	115.1	FA	175.7(5)	C(77)-C(78)-C(70)	122.1	O(2A)-N(2)-C(95)	119.1
C(82)-C(81)-C(86)	119.1	HA	177.4(8)	C(92)-C(91)-C(96)	119.1	CA	165.0(6)
C(82)-C(81)-C(4)	121.1	C(78)-C(70)-C(74)	116.1				
Complex 7b							
Distances							
Ru-C*	1.95(2)	P(1)-C(21)	1.88(2)	Δ	0.22(2)	C(72)-C(73)	1.42(3)
Ru-C(1)	1.99(2)	P(1)-C(31)	1.80(2)	C(1)-C(2)	1.19(3)	C(73)-C(74)	1.33(3)
Ru-P(1)	2.307(6)	P(2)-C(41)	1.84(3)	C(2)-C(3)	1.38(3)	C(74)-C(75)	1.40(2)
Ru-P(2)	2.300(8)	P(2)-C(51)	1.84(2)	C(3)-C(4)	1.35(2)	C(75)-C(76)	1.39(3)
Ru-C(70)	2.44(2)	P(2)-C(61)	1.85(2)	C(4)-C(5)	1.35(3)	C(76)-C(77)	1.39(3)
Ru-C(71)	2.19(2)	C(81)-C(86)	1.39(3)	C(5)-C(6)	1.34(3)	C(77)-C(78)	1.34(3)
Ru-C(72)	2.17(2)	C(84)-N	1.50(3)	C(6)-C(81)	1.44(3)	C(81)-C(82)	1.46(3)
Ru-C(73)	2.20(2)	C(82)-C(83)	1.36(3)	C(70)-C(78)	1.33(3)	C(83)-C(84)	1.33(3)
Ru-C(74)	2.40(2)	C(84)-C(85)	1.35(2)	C(70)-C(74)	1.45(3)	C(85)-C(86)	1.36(3)
P(1)-C(11)	1.89(2)	N-O(1)	1.20(2)	C(70)-C(71)	1.41(3)	N-O(2)	1.17(3)
Angles							
C*-Ru-P(1)	124.5(7)	C(5)-C(6)-C(81)	130.2	C(78)-C(70)-C(74)	123.2	C(70)-C(78)-C(77)	121.3
C*-Ru-P(2)	121.3(7)	C(86)-C(81)-C(6)	123.2	C(78)-C(70)-C(71)	136.3	C(78)-C(77)-C(76)	119.3
C*-Ru-C(1)	122.1	C(6)-C(81)-C(82)	122.2	C(71)-C(70)-C(74)	100.2	C(86)-C(81)-C(82)	114.2
C(1)-Ru-P(1)	85.4(7)	C(84)-C(83)-C(82)	120.3	C(72)-C(71)-C(70)	117.3	C(83)-C(82)-C(81)	120.3
C(1)-Ru-P(2)	88.4(7)	C(83)-C(84)-N	116.2	C(71)-C(72)-C(73)	100.3	C(83)-C(84)-C(85)	125.3
P(2)-Ru-P(1)	104.3(2)	C(84)-C(85)-C(86)	116.3	C(74)-C(73)-C(72)	114.2	C(85)-C(84)-N	119.3
C(2)-C(1)-Ru	172.2	O(2)-N-O(1)	124.3	C(75)-C(74)-C(70)	115.2	C(85)-C(86)-C(81)	125.2
C(1)-C(2)-C(3)	178.3	O(1)-N-C(84)	119.3	C(73)-C(74)-C(75)	135.3	O(2)-N-C(84)	116(3)
C(4)-C(3)-C(2)	130.2	FA	174.1	C(73)-C(74)-C(70)	109.2	CA	161.1
C(6)-C(5)-C(4)	128.2	HA	177.2	C(76)-C(75)-C(74)	119.3	DA	7.6(9)
C(3)-C(4)-C(5)	127.2						

^a $D = d[\text{Ru}-\text{C}(74), \text{C}(70)] - d[\text{Ru}-\text{C}(71), \text{C}(73)]$. ^b FA (fold angle) = angle between normals to least-squares planes defined by C(71), C(72), C(73) and C(70), C(74), C(75), C(76), C(77), C(78). ^c HA (hinge angle) = angle between normals to least-squares planes defined by C(71), C(72), C(73) and C(71), C(74), C(70), C(73). ^d CA (conformational angle) = angle between normals to least-squares planes defined by C*, C*, Ru and C*, Ru, P(2). ^e DA = angle between normals to least-squares planes defined by C*, Ru, C(1) and Ru, C(1), C(2), C(3), C(4), C(5), C(6), C(81), C(82), C(83), C(84), C(85), C(86), N, O(1), O(2). (Deviations of the atoms from the plane (Å): Ru: -0.0108; C(1): 0.0093; C(2): 0.1068; C(3): 0.2515; C(4): 0.1680; C(5): 0.2056; C(6): 0.0964; C(81): 0.0878; C(82): 0.0757; C(83): 0.0397; C(84): -0.0160; C(85): 0.0122; C(86): 0.0805; N: -0.0808; O(1): -0.1506; O(2): -0.2448). C* = centroid of C(70), C(71), C(72), C(73), C(74). C** = centroid of C(70), C(74), C(75), C(76), C(77), C(78).

(β). It is worth mentioning that studies concerning bimetallic complexes possessing second-order NLO properties are scarce.^{4f,16}

Since the $\text{C}\equiv\text{N}$ group is one of the most simple and efficient unsaturated bridging groups the precursor complex $[\text{Ru}(\text{C}\equiv\text{N})(\eta^5-\text{C}_9\text{H}_7)(\text{PPh}_3)_2]$ (**10**) was prepared (81% yield), as an appropriate precursor of dinuclear

species by reaction of **1a** with KCN in refluxing methanol (Scheme 5). The IR spectrum shows the expected $\nu(\text{C}\equiv\text{N})$ absorption band at 2071 cm^{-1} , and the $^{13}\text{C}\{^1\text{H}\}$ NMR spectrum exhibits the $\text{Ru}-\text{C}\equiv\text{N}$ resonance, which appears as a triplet at δ 143.49 ppm ($^2J_{\text{CP}} = 22.7\text{ Hz}$).

As expected, the cyano group acts in complex **10** as a good bridging ligand which allows the synthesis of

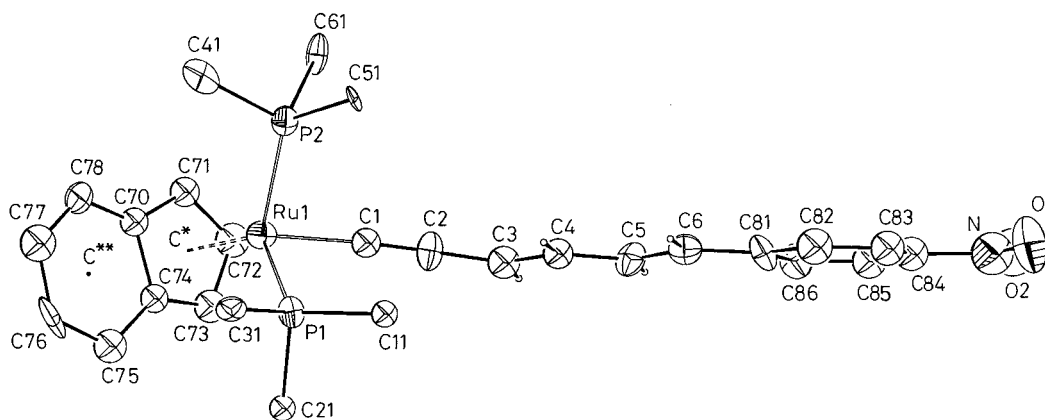
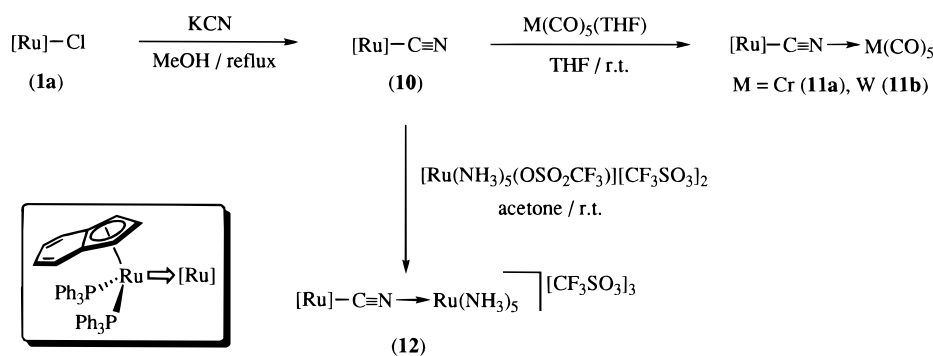


Figure 3. ORTEP view of the structure of complex **9** showing the planarity of the dienynyl chain and the nitroaryl ring.

Scheme 5



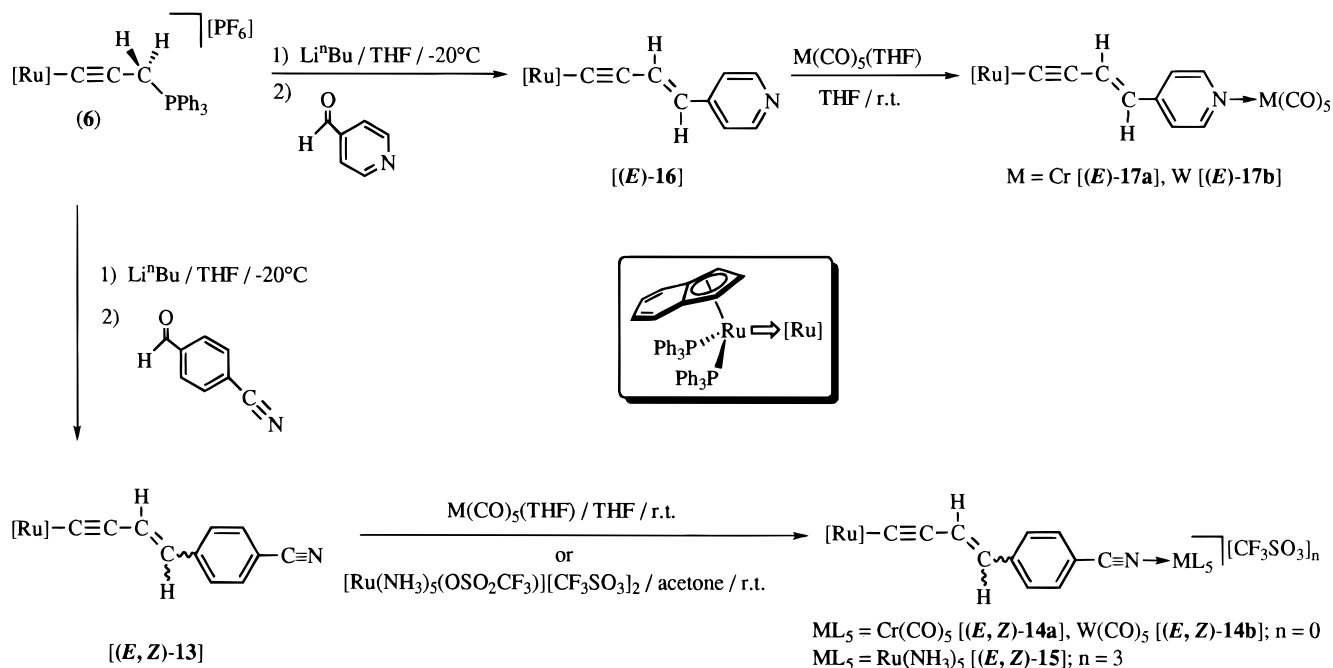
dinuclear metal complexes. Thus, the reaction of compound **10** with an equimolar amount of $[M(\text{CO})_5(\text{THF})]$ ($M = \text{Cr}, \text{W}$) in THF, at room temperature, yields the neutral bimetallic derivatives $[(\eta^5\text{-C}_9\text{H}_7)(\text{PPh}_3)_2\text{Ru}\{\mu\text{-C}\equiv\text{N}\}M(\text{CO})_5]$ (**11a,b**) (70 and 85% yield, respectively) (Scheme 5). IR and NMR data support the proposed formulations (see Experimental Section for details). Thus, IR spectra show typical $\nu(\text{C}\equiv\text{N})$ and $\nu(\text{C}=\text{O})$ absorptions in the range 1881–2109 cm^{-1} , and the $^{13}\text{C}\{-^1\text{H}\}$ NMR spectra display $\text{Ru}\text{-C}\equiv\text{N}$ triplet resonances at δ 155.97 ($^2J_{\text{CP}} = 20.7$ Hz) (**11a**) and 154.80 ppm ($^2J_{\text{CP}} = 20.6$ Hz) (**11b**). Downfield $M\text{-CO}$ singlet resonances were also observed in the range δ 198.18–220.76 ppm. Similarly, the treatment of **10** with $[\text{Ru}(\text{NH}_3)_5(\text{OSO}_2\text{CF}_3)][\text{CF}_3\text{SO}_3]_2$ generates the cationic $\text{Ru}^{\text{II}}\text{-Ru}^{\text{III}}$ bimetallic derivative $[(\eta^5\text{-C}_9\text{H}_7)(\text{PPh}_3)_2\text{Ru}\{\mu\text{-C}\equiv\text{N}\}\text{Ru}(\text{NH}_3)_5][\text{CF}_3\text{SO}_3]_3$ (**12**) which was characterized by elemental analysis, conductivity measurements and IR spectroscopy (see Scheme 5 and Experimental Section).

Mixed valence bimetallic derivatives were also synthesized starting from the σ -enynyl complexes $[\text{Ru}(\text{C}\equiv\text{CCH}=\text{CH}-\text{C}_6\text{H}_4\text{CN}-4)(\eta^5\text{-C}_9\text{H}_7)(\text{PPh}_3)_2]$ (**13**) and $[\text{Ru}(\text{C}\equiv\text{CCH}=\text{CH}-\text{C}_5\text{H}_4\text{N}-4)(\eta^5\text{-C}_9\text{H}_7)(\text{PPh}_3)_2]$ (**16**) which bear uncoordinated cyano or pyridine terminal groups. These complexes were prepared through Wittig-type reactions as described above for the analogous σ -enynyl compounds **7–9** (Scheme 6). It is worth mentioning that while **13** was obtained as a nonseparable mixture of the *E* and *Z* stereoisomers (ca. 4/1, 71% yield), complex **16** was surprisingly obtained stereoselectively as the *E* stereoisomer (83% yield). Their analytical and spectroscopic data, which are similar to those of σ -enynyl complexes **7–9** (see Experimental Section and Tables 1 and 2), are consistent with the proposed formulations.

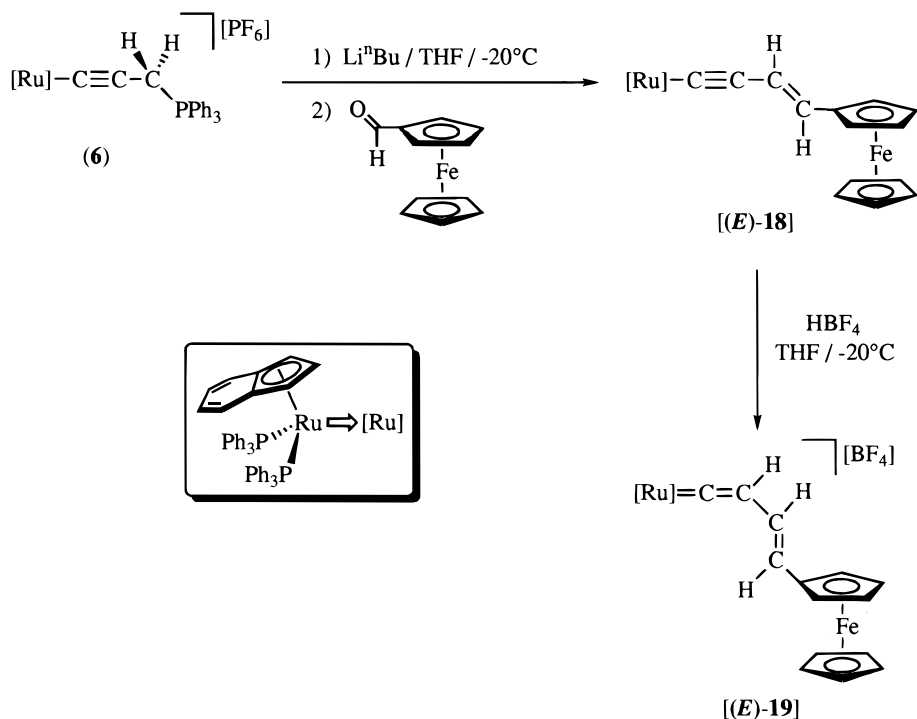
Treatment of **13** and **16** with $[M(\text{CO})_5(\text{THF})]$ ($M = \text{Cr}, \text{W}$) leads to the formation of the neutral bimetallic complexes **14a,b** and **17a,b**, respectively (70–85% yield) (Scheme 6) which were characterized by microanalyses, IR, and NMR spectroscopy (see Experimental Section and Tables 1 and 2). Significantly, the NMR spectra show the expected proton and carbon resonances at similar chemical shifts to those shown in the spectra of the precursor complexes **13** and **16**, indicating a small electronic effect upon the coordination to the $M(\text{CO})_5$ fragment. The cationic $\text{Ru}^{\text{II}}\text{-Ru}^{\text{III}}$ bimetallic derivative **15** was similarly prepared from **13** by the reaction with $[\text{Ru}(\text{NH}_3)_5(\text{OSO}_2\text{CF}_3)][\text{CF}_3\text{SO}_3]_2$ as is described above for the analogous dinuclear complex **12** (53% yield) (Scheme 6). Complexes **14a,b** and **15** have been isolated as a mixture of the corresponding stereoisomers *E* and *Z* in accordance with the isomeric mixture of the precursor derivative **13**.

Bimetallic Ruthenium(II)–Iron(II) Complexes
 $[\text{Ru}(\text{C}\equiv\text{CCH}=\text{CH}-\text{C}_5\text{H}_4\text{FeC}_5\text{H}_5)(\eta^5\text{-C}_9\text{H}_7)(\text{PPh}_3)_2]$ [**(E)-18**] and $[\text{Ru}\{\text{-C}=\text{C}(\text{H})-\text{CH}=\text{CH}-\text{C}_5\text{H}_4\text{FeC}_5\text{H}_5\}(\eta^5\text{-C}_9\text{H}_7)(\text{PPh}_3)_2][\text{BF}_4]$ [**(E)-19**]. Since the ferrocenyl group $(\eta^5\text{-C}_5\text{H}_4)\text{Fe}(\eta^5\text{-C}_5\text{H}_5)$ has been widely used in organometallic complexes with NLO properties, it was of interest to synthesize a bimetallic complexes involving this group as part of the π -conjugated system.⁴ The synthesis of the novel ferrocenyl complex was achieved through the Wittig-type reaction between the alkynylphosphonio complex **6** and ferrocenecarboxaldehyde. The reaction is stereoselective affording the bimetallic complex $[\text{Ru}(\text{C}\equiv\text{CCH}=\text{CHC}_5\text{H}_4\text{FeC}_5\text{H}_5)(\eta^5\text{-C}_9\text{H}_7)(\text{PPh}_3)_2]$ [**(E)-18**] isolated as a red crystalline solid (67% yield) (Scheme 7). $^{31}\text{P}\{^1\text{H}\}$, ^1H , and $^{13}\text{C}\{^1\text{H}\}$ NMR spectra reveal typical signals of both $[\text{Ru}(\eta^5\text{-C}_9\text{H}_7)(\text{PPh}_3)_2]$ and

Scheme 6



Scheme 7



$[\eta^5\text{-C}_5\text{H}_4\text{Fe}(\eta^5\text{-C}_5\text{H}_5)]$ moieties along with resonances assigned to the enynyl bridging chain. The coupling constant ($J_{\text{HH}} = 15.7$ Hz) for the olefinic protons in the ^1H NMR spectrum clearly indicates an *E* configuration of the carbon-carbon double bond. Protonation of *(E)*-**18** takes place regioselectively on the C_β atom of the alkynyl group, yielding the cationic vinyl-vinylidene complex $[\text{Ru}\{\text{C}=\text{C}(\text{H})\text{CH}=\text{CHC}_5\text{H}_4\text{FeC}_5\text{H}_5\}(\eta^5\text{-C}_9\text{H}_7)(\text{PPh}_3)_2][\text{BF}_4]$ [*(E)*-**19**] (71% yield) (Scheme 7). The presence of the vinylidene moiety was identified, as usual, on the basis of (i) (^1H NMR) a broad singlet resonance at δ 5.34 ppm for the $\text{Ru}=\text{C}=\text{CH}$ proton and

(ii) (^{13}C NMR) the low-field triplet resonance of the carbene carbon $\text{Ru}=\text{C}_\alpha$ (361.82 ppm, $^2J_{\text{CP}} = 16.5$ Hz).

Quadratic Hyperpolarizabilities. The molecular hyperpolarizabilities of complexes **2–5** and **7–19** as determined by the hyper-Rayleigh scattering (HRS) technique are given in Table 4. Comparison of **3–5** and **7** with organic amino analogues shows that despite the triple carbon-carbon bond the half sandwich $[\text{Ru}]-\text{C}\equiv\text{C}$ moiety is a powerful donor that can compete with the strongest organic donors.^{2b,c,18,19} It has been suggested that the high effectiveness of this indenylruthenium-(II) donor fragment compared to other organometallic

Table 4. Wavelength of Maximum Absorptions and First Hyperpolarizabilities for Complexes 2–19^a

complex	λ_{max} (nm)	β ($\times 10^{-30}$ esu) ^b	β_0 ($\times 10^{-30}$ esu) ^b
2a	379	116	50
3a	476	746	119
3b	459	516	107
3c	456	540	117
4	463	1027	202
5	509	1295	85
(E,Z)-7a	507	1257	89
(EE,ZE)-7b	523	1320	34
(E,Z)-8a	550	908	43
(E)-8b	598	487	88
9	345	48	25
10	396	13	5
11a	392	25	10
11b	392	40	15
12*	621	108	26
(E,Z)-13	427	238	71
(E,Z)-14a	442	465	119
(E,Z)-14b	456	700	150
(E,Z)-15*	442	315	80
(E)-16	399	100	37
(E)-17a	451	260	60
(E)-17b	462	535	71
(E)-18	345	273	141
(E)-19	301	117	73

^a Recorded in dichloromethane except for * (acetone solutions).

^b The hyper-Rayleigh scattering measurements were performed at 1064 nm; all values $\pm 10\%$; the static values β_0 are calculated using the two-level model.

species such as ferrocenes originates from the in-plane MLCT transition (MLCT lies in the plane formed by the conjugated system), unlike to the out-of-plane MLCT transition present in metallocenes (MLCT axis is perpendicular to the plane formed by the conjugated system).^{3c,4c,7a,18} Although part of the large NLO efficiency of these complexes is attributed to resonance enhancement, the calculated static hyperpolarizabilities (β_0) still confirm this tendency.

Within the series studied, changes induced in the phosphine ligand (**3a–c**) do not have an impact on the static hyperpolarizability. Although there are no differences in the hyperpolarizability between **4** and **5** and their cyclopentadienyl counterparts [Ru(η^5 -C₅H₅)(PPh₃)₂] reported by Humphrey and co-workers ($\beta_0 = 202$ vs 212×10^{-30} and 85 vs 86×10^{-30} esu, respectively),^{3c} the value found for **3a** (119 vs 96×10^{-30} esu)^{3c} seems to indicate that the indenyl group is only slightly more effective than the cyclopentadienyl ring in increasing the electron donor capability of the ruthenium center. Chain lengthening of the organic ligands (compare **3–5** and **7** and **8**) results in a clear increase of the measured hyperpolarizability, yet the calculated static values do not confirm this trend. Since the two-level model has been originally introduced for molecules showing only one transition, this may indicate that the model is inadequate for the complexes investigated in this work. However, the good results obtained with the two-level model for other linear organometallic compounds with the MLCT transition as the main contributor to the hyperpolarizability is a good indication that the failure of the model originates from the neglect of the damping

(17) The parameter $\Delta\delta(\text{C-3a,7a})$ can be used as an indication of the indenyl distortion: (a) Baker, R. T.; Tulip, T. H. *Organometallics* **1986**, *5*, 839. (b) Kohler, F. G. *Chem. Ber.* **1974**, *107*, 570.

(18) Verbiest, T.; Houbrechts, S.; Kauranen, M.; Clays, K.; Persoons, A. *J. Mater. Chem.* **1997**, *7*, 2175.

(19) Matsuzawa, N.; Dixon, D. A. *J. Phys. Chem.* **1992**, *96*, 6232.

term which leads to an underestimated static value for compounds with their MLCT band close to the harmonic frequency (532 nm).^{7d–9,16a,20} The shortcoming of the two-level model and the presence of strong resonance enhancement for **5–8** prohibit any presumptions on their relative NLO efficiencies. Nevertheless, the results for **7a,b** seem to suggest the hyperpolarizability levels off upon the addition of the second double bond. The low hyperpolarizabilities for **2a** with respect to **3a** emanates most likely from the net positive charge on the ruthenium center which results in a decrease of the electron donor ability of the [Ru]^{+=C=C} metal fragment as compared to that of [Ru]–C \equiv C. Furthermore, the rather low hyperpolarizability of **9** indicates that the increased π -system is insufficient to account for the loss of β as the acceptor *p*-NO₂ group is replaced by the two *m*-NO₂ groups.²

The hyperpolarizabilities of bimetallic complexes **10–19** have also been assessed. The addition of a metal group to a cyano or pyridyl acceptor in the series **10–12**, **13–15**, and **16,17** has been found to increase the NLO effectivity of the monometallic precursor complex (**10**, **13**, and **16**). Previous reports on pyridylmetal pentacarbonyl complexes by Kanis et al. suggested that the role of the metal is limited to that of an inductive acceptor that lowers the energy of the pyridyl-centered LUMO.²¹ The pyridyl ring itself remains the effective molecular acceptor. If we assume that this mechanism is also valid for the cyano complexes studied here, then the differences observed between the bimetallic compounds and their precursor complexes can be explained by the different σ acceptor effectiveness of the attached metal groups. It is expected that the tungsten complexes (**11b**, **14b**, and **17b**) should have larger hyperpolarizabilities than their chromium analogues (**11a**, **14a**, and **17a**) since the electron density at the tungsten center is better reduced by the π back-donation to the carbonyl groups.²² A comparison of the Ru(II)–Ru(III) complexes (**12** and **15**) and the Ru(II)–group 6 metal complexes (**11** and **14**) is not so straightforward as an inverse order is observed in both series. Theoretical calculations may be needed to reveal which has the largest influence on the LUMO, either the higher intrinsic electronegativity of the Ru(III) center with respect to W(0) and Cr(0) or the presence of the donor NH₃ ligands as compared to the π acceptor CO ligands. Note that the group 6 metal cyanobenzene and pyridyl complexes **14**, **15**, and **17** exhibit the largest hyperpolarizabilities found for bimetallic complexes to date.^{3,18}

Complexes **18** and **19** contain two metal groups which have both previously been used as an electron donor and thus display a *D*₁- π -*D*₂ symmetry. A previous study by Colbert et al. on similar chiral bimetallic ferrocene

(20) (a) Coe, B. J.; Chadwick, G.; Houbrechts, S.; Persoons, A. *J. Chem. Soc., Dalton Trans.* **1997**, 1705. (b) Coe, B. J.; Chamberlain, M. C.; Essex-Lopresti, J. P.; Gaines, S.; Jeffery, J. C.; Houbrechts, S.; Persoons, A. *Inorg. Chem.* **1997**, *36*, 3284. (c) Coe, B. J.; Essex-Lopresti, J. P.; Houbrechts, S.; Persoons, A. *Chem. Commun.* **1997**, 1645. (d) Coe, B. J.; Harris, J. A.; Harrington, L. J.; Jeffery, J. C.; Rees, L. H.; Houbrechts, S.; Persoons, A. *Inorg. Chem.* **1998**, *37*, 3391.

(21) (a) Kanis, D. R.; Ratner, M. A.; Marks, T. J. *Chem. Rev.* **1994**, *94*, 195. (b) Kanis, D. R.; Lacroix, P. G.; Ratner, M. A.; Marks, T. J. *J. Am. Chem. Soc.* **1994**, *116*, 10089.

(22) (a) Crabtree, R. H. *The Organometallic Chemistry of the Transition Metals*; Wiley-Interscience: New York, 1994; p 13. (b) It has also been reported that the value of β also decreases for chromium Fischer-type carbene complexes as compared with the analogous tungsten complexes. See ref 5c.

complexes only revealed negligible NLO properties.²³ Therefore, the large hyperpolarizabilities found here are rather unexpected. The results suggest that the donor strength of both groups is sufficiently different to induce the molecular asymmetry required for good NLO properties.

Concluding Remarks

In this work we describe the synthesis of novel donor–acceptor ruthenium(II) complexes which show excellent NLO properties. Through efficient synthetic methodologies, complexes of the following types have been prepared in good yields: (a) σ -arylacetylruthenium(II) complexes (**3–5**), (b) σ -enynyl- and σ -dienynylruthenium(II) complexes (**7–9**, **13**, **16**), and (c) bimetallic ruthenium(II)–chromium(0) (**11a**, **14a**, **17a**), ruthenium(II)–tungsten(0) (**11b**, **14b**, **17b**), ruthenium(II)–ruthenium(III) (**12**, **15**), and ruthenium(II)–iron(II) complexes (**18**, **19**). Most of these complexes are characterized by the presence of a formal donor indenylruthenium(II) moiety $[\text{Ru}(\eta^5\text{-C}_9\text{H}_7)\text{L}_2]$ and a strong π acceptor group such as the NO_2 group or a metal carbonyl fragment. Novel derivatives also include mild donor–acceptor systems such as Ru(II)–Fe(II) and the mixed valence Ru(II)–Ru(III) pair. In these complexes the donor and acceptor centers are linked either by a π -conjugated hydrocarbon system (i.e., aryacylylide $-\text{C}\equiv\text{C}-\text{C}_6\text{H}_4-$, $-\text{C}\equiv\text{C}-\text{C}_6\text{H}_4-\text{C}\equiv\text{C}-\text{C}_6\text{H}_4-$ or $-\text{C}\equiv\text{C}-\text{C}_6\text{H}_4-\text{N}=\text{CH}-\text{C}_6\text{H}_4-$; enynyl $-\text{C}\equiv\text{C}-\text{CH}=\text{CH}-\text{C}_6\text{H}_4-$ or $-\text{C}\equiv\text{C}-\text{CH}=\text{CH}-\text{C}_4\text{H}_2\text{X}-$; dienynyl $-\text{C}\equiv\text{C}-(\text{CH}=\text{CH})_2-\text{C}_6\text{H}_4-$) or by a N-functionalized bridge (i.e., cyanide group $-\text{C}\equiv\text{N}-$ or $-\text{C}\equiv\text{C}-\text{CH}=\text{CH}-\text{C}_6\text{H}_4-\text{C}\equiv\text{N}-$; pyridyl group $-\text{C}\equiv\text{C}-\text{CH}=\text{CH}-\text{C}_5\text{H}_4\text{N}-$). All of these unsaturated skeletons enable the electronic communication between the donor and acceptor fragments (metal-to-ligand charge transfer (MLCT)). This is assessed by means of the X-ray crystal structure of the complex $[\text{Ru}\{\text{C}\equiv\text{C}-(\text{CH}=\text{CH})_2-\text{C}_6\text{H}_4\text{NO}_2-4\}(\eta^5\text{-C}_9\text{H}_7)(\text{PPh}_3)_2]$ (**7b**) which shows the planarity of the hydrocarbon chain in such a way that all of the π orbitals of the conjugated system, including those of the aryl ring, are able to perform a favorable overlapping.^{15c}

Determination of molecular quadratic hyperpolarizabilities (β) (HRS) for these donor–acceptor derivatives yields resonantly enhanced values significantly larger than those of the more commonly studied organometallic chromophores ($\beta_{1064\text{ nm}} = 100\text{--}1320 \times 10^{-30}$ esu). Most significantly, the complexes **14**, **15**, and **17** show the largest static quadratic hyperpolarizabilities values ($\beta_0 = 10\text{--}150 \times 10^{-30}$ esu) found for bimetallic complexes to date.

In summary, we describe an accessible entry to organotransition metal complexes of interest as new materials for nonlinear optics. Some of these complexes show β values which are among the highest reported for organometallic complexes, representing good examples for the still very scarce information on the relationship between the molecular structures and NLO properties. In this regard MO calculations to determine the nature of the LUMO orbitals in these type of donor–acceptor complexes may be of interest. Theoretical

studies aimed at a better understanding of the influence of the acceptor group and the π -conjugated bridging system on the hyperpolarizability values in these ruthenium(II) complexes are in progress.

Experimental Section

The manipulations were performed in an atmosphere of dry nitrogen using vacuum-line and standard Schlenk techniques. All reagents were obtained from commercial suppliers and used without further purification. Solvents were dried by standard methods and distilled under nitrogen before use. The compounds $[\text{RuCl}(\eta^5\text{-C}_9\text{H}_7)\text{L}_2]$ ($\text{L}_2 = 2\text{PPh}_3$,²⁴ **dppe**,²⁵ **dppm**²⁵), $[\text{Ru}(\text{NH}_3)_5(\text{OSO}_2\text{CF}_3)][\text{CF}_3\text{SO}_3]_2$,²⁶ $\text{HC}\equiv\text{C}-\text{C}_6\text{H}_4\text{NO}_2-4$,²⁷ and $\text{HC}\equiv\text{C}-\text{C}_6\text{H}_4\text{R}-4$ ($\text{R} = \text{C}\equiv\text{C}-\text{C}_6\text{H}_4\text{NO}_2-4$,²⁸ $\text{N}=\text{CH}-\text{C}_6\text{H}_4\text{NO}_2-4$ ^{7a}) were prepared by following the methods reported in the literature.

Infrared spectra were recorded on a Perkin-Elmer 1720-XFT spectrometer. The conductivities were measured at room temperature, in ca. 10^{-3} mol dm⁻³ acetone solutions, with a Jenway PCM3 conductimeter. The C, H, and N analyses were carried out with a Perkin-Elmer 240-B microanalyzer. Non satisfactory microanalyses were obtained for complexes **5** and **8a,b**, due to uncompleted combustions, instead mass spectra (FAB) were recorded for these complexes using a VG Autospec spectrometer, operating in the positive mode; 3-nitrobenzyl alcohol was used as the matrix. UV–vis spectra were recorded using a Shimadzu UV-160 spectrophotometer. NMR spectra were recorded on a Bruker AC300 instrument at 300 MHz (¹H), 121.5 MHz (³¹P) or 75.4 MHz (¹³C) using SiMe₄ or 85% H₃PO₄ as standards. DEPT experiments have been carried out for all of the complexes. ³¹P{¹H}, ¹H, and ¹³C{¹H} NMR spectroscopic data for the donor–acceptor σ alkynyl complexes are collected in Tables 1 and 2.

Synthesis of $[\text{Ru}\{\text{C}=\text{C}(\text{H})-\text{C}_6\text{H}_4\text{NO}_2-4\}(\eta^5\text{-C}_9\text{H}_7)\text{L}_2][\text{PF}_6]$ ($\text{L}_2 = 2\text{PPh}_3$ (2a**), **dppe** (**2b**), **dppm** (**2c**)).** **General Procedure.** A mixture of $[\text{RuCl}(\eta^5\text{-C}_9\text{H}_7)\text{L}_2]$ (**1a–c**) (1 mmol), NaPF₆ (0.336 g, 2 mmol), and $\text{HC}\equiv\text{C}-\text{C}_6\text{H}_4\text{NO}_2-4$ (0.294 g, 2 mmol) in 50 mL of methanol was heated under reflux for 2 h. The resulting solution was evaporated to dryness, and the solid residue was dissolved in dichloromethane (ca. 20 mL) and filtered into stirred diethyl ether (ca. 100 mL) to give a brown solid precipitate. The resulting solid was washed with diethyl ether (2 \times 20 mL) and vacuum-dried. Yield, IR (KBr, $\nu(\text{PF}_6^-)$, cm⁻¹), analytical data, conductivity (acetone, Ω^{-1} cm² mol⁻¹), and NMR spectroscopic data (ppm) are as follows. For **2a**. 67% (0.692 g). 839. Anal. Calcd for RuC₅₃H₄₂F₆P₃O₂N: C, 61.63; H, 4.10; N, 1.35. Found: C, 62.22; H, 4.12; N, 1.31. 115. ³¹P{¹H} (CDCl₃) δ 37.72 (s); ¹H (CDCl₃) δ 5.34 (t, 1H, ⁴J_{HP} = 1.5 Hz, Ru=C=CH), 5.72 (d, 2H, ³J_{HH} = 2.6 Hz, H-1,3), 6.04 (m, 3H, H-2 and H-4,7 or H-5,6), 6.82–7.48 (m, 34H, Ph, H-4,7 or H-5,6 and C₆H₂H₂NO₂-4), 7.91 (d, 2H, ³J_{HH} = 8.8 Hz, C₆H₂H₂NO₂-4); ¹³C{¹H} (CDCl₃) δ 84.59 (s, C-1,3), 98.75 (s, C-2), 116.43 (s, C-3a,7a), 117.49 (s, C _{β}), 123.75, 124.31 and 126.61 (s, C-4,7, C-5,6 and CH of C₆H₄NO₂-4), 128.68–133.98 (m, Ph and CH of C₆H₄NO₂-4), 136.75 and 146.21 (s, C of C₆H₄NO₂-4), 348.98 (t, ²J_{CP} = 16.5 Hz, Ru=C _{α}); $\Delta\delta(\text{C-3a,7a}) = -14.27$. For **2b**. 52% (0.471 g). 837. Anal. Calcd for RuC₄₃H₃₆F₆P₃O₂N: C, 56.95; H, 4.00; N, 1.54. Found: C, 57.35; H, 4.18; N, 1.72. 108. ³¹P{¹H} (CDCl₃) δ 71.66 (s); ¹H (CDCl₃) δ 2.44 and 2.84 (m, 2H each one, P(CH₂)₂P), 4.38 (s, 1H, Ru=C=CH), 5.95 (t, 1H, ³J_{HH} =

(24) Oro, L. A.; Ciriano, M. A.; Campo, M.; Foces-Foces, C.; Cano, F. H. *J. Organomet. Chem.* **1985**, *289*, 117.

(25) Gamasa, M. P.; Gimeno, J.; González-Bernardo, C.; Martín-Vaca, B. M.; Monti, D.; Bassetti, M. *Organometallics* **1996**, *15*, 302.

(26) Lawrence, G. A.; Lay, P. A.; Sargeson, A. M.; Taube, H. *Inorg. Synth.* **1986**, *24*, 258.

(27) Takahashi, S.; Kuroyama, Y.; Sonogashira, K.; Hagihara, N. *Synthesis* **1980**, 627.

(28) (a) Lavastre, O.; Cabioch, S.; Dixneuf, P. H.; Vohlidal, J. *Tetrahedron* **1997**, *53*, 7595. (b) Lavastre, O.; Ollivier, L.; Dixneuf, P. H.; Sibandhit, S. *Tetrahedron* **1996**, *52*, 5495.

(23) Colbert, M. C. B.; Lewis, J.; Long, N. J.; Raithby, P. R.; Bloor, D. A.; Cross, G. H. *J. Organomet. Chem.* **1997**, *531*, 183.

2.2 Hz, H-2), 6.14 (d, 2H, $J_{\text{HH}} = 2.2$ Hz, H-1,3), 6.30 and 7.62 (d, 2H each one, $J_{\text{HH}} = 8.7$ Hz, $\text{C}_6\text{H}_4\text{NO}_2$ -4), 6.69–7.52 (m, 24H, Ph, H-4,7 and H-5,6); $^{13}\text{C}\{^1\text{H}\}$ (CDCl_3) δ 25.81 (m, $\text{P}(\text{CH}_2)_2\text{P}$), 79.75 (s, C-1,3), 97.96 (s, C-2), 113.23 (s, C-3a,7a), 115.36 (s, C_β), 123.24, 123.52 and 124.96 (s, C-4,7, C-5,6 and CH of $\text{C}_6\text{H}_4\text{NO}_2$ -4), 129.16–133.43 (m, Ph and CH of $\text{C}_6\text{H}_4\text{NO}_2$ -4), 135.00 and 145.14 (s, C of $\text{C}_6\text{H}_4\text{NO}_2$ -4), 348.85 (t, $^2J_{\text{CP}} = 16.5$ Hz, $\text{Ru}=\text{C}_\alpha$); $\Delta\delta(\text{C-3a,7a}) = -17.47$. For **2c**. 49% (0.437 g). 834. Anal. Calcd for $\text{RuC}_{42}\text{H}_{34}\text{F}_6\text{P}_3\text{O}_2\text{N}$: C, 56.50; H, 3.83; N, 1.56. Found: C, 55.92; H, 3.75; N, 1.48. $^{31}\text{P}\{^1\text{H}\}$ (CDCl_3) δ 1.69 (s); ^1H (CDCl_3) δ 4.57 (s, 1H, $\text{Ru}=\text{C}=\text{CH}$), 4.74 and 5.10 (m, 1H each one, $\text{PCH}_2\text{H}_2\text{P}$), 5.86 (t, 1H, $J_{\text{HH}} = 2.5$ Hz, H-2), 6.33 (m, 4H, H-1,3 and H-4,7 or H-5,6), 7.10–7.44 (m, 24H, Ph, H-4,7 or H-5,6 and $\text{C}_6\text{H}_2\text{H}_2\text{NO}_2$ -4), 7.66 (d, 2H, $J_{\text{HH}} = 8.6$ Hz, $\text{C}_6\text{H}_2\text{H}_2\text{NO}_2$ -4); $^{13}\text{C}\{^1\text{H}\}$ (CDCl_3) δ 45.62 (t, $J_{\text{CP}} = 29.0$ Hz, PCH_2P), 80.69 (s, C-1,3), 95.81 (s, C-2), 111.92 (s, C-3a,7a), 117.62 (s, C_β), 124.14, 124.61, 126.02 and 128.82 (s, C-4,7, C-5,6 and CH of $\text{C}_6\text{H}_4\text{NO}_2$ -4), 129.62–133.70 (m, Ph), 135.83 and 145.93 (s, C of $\text{C}_6\text{H}_4\text{NO}_2$ -4), 352.42 (t, $^2J_{\text{CP}} = 14.7$ Hz, $\text{Ru}=\text{C}_\alpha$); $\Delta\delta(\text{C-3a,7a}) = -18.78$.

Synthesis of $[\text{Ru}(\text{C}\equiv\text{C}-\text{C}_6\text{H}_4\text{NO}_2\text{-4})(\eta^5\text{-C}_9\text{H}_7)\text{L}_2]$ ($\text{L}_2 = 2\text{PPh}_3$ (3a**), dppe (**3b**), dppm (**3c**)).** General Procedure.

A solution of **2a–c** (1 mmol) in 50 mL of dichloromethane was treated with Al_2O_3 (1.019 g, 10 mmol), and the mixture was stirred at room temperature for 1 h. The solution was then evaporated to dryness, and the solid residue was extracted with diethyl ether. The evaporation of the diethyl ether gave **3a–c** as red solids. Yield, IR (KBr, $\nu(\text{C}\equiv\text{C})$, cm^{-1}), and analytical data are as follows. For **3a**. 79% (0.701 g). 2051. Anal. Calcd for $\text{RuC}_{53}\text{H}_{41}\text{P}_2\text{O}_2\text{N}$: C, 71.77; H, 4.66; N, 1.58. Found: C, 70.95; H, 4.33; N, 1.62. For **3b**. 68% (0.507 g). 2060. Anal. Calcd for $\text{RuC}_{43}\text{H}_{35}\text{P}_2\text{O}_2\text{N}$: C, 67.88; H, 4.64; N, 1.84. Found: C, 67.25; H, 4.58; N, 1.69. For **3c**. 42% (0.314 g). 2052. Anal. Calcd for $\text{RuC}_{42}\text{H}_{33}\text{P}_2\text{O}_2\text{N}$: C, 67.56; H, 4.45; N, 1.87. Found: C, 66.97; H, 4.46; N, 1.80.

Synthesis of $[\text{Ru}(\text{C}\equiv\text{C}-\text{C}_6\text{H}_4\text{R-4})(\eta^5\text{-C}_9\text{H}_7)(\text{PPh}_3)_2]$ ($\text{R} = \text{C}\equiv\text{C}-\text{C}_6\text{H}_4\text{NO}_2\text{-4}$ (4**), $\text{N}=\text{CH}-\text{C}_6\text{H}_4\text{NO}_2\text{-4}$ (**5**)).** A mixture of $[\text{RuCl}(\eta^5\text{-C}_9\text{H}_7)(\text{PPh}_3)_2]$ (**1a**) (0.776 g, 1 mmol), NaPF_6 (0.336 g, 2 mmol), and $\text{HC}\equiv\text{C}-\text{C}_6\text{H}_4\text{R-4}$ ($\text{R} = \text{C}\equiv\text{C}-\text{C}_6\text{H}_4\text{NO}_2\text{-4}$ or $\text{N}=\text{CH}-\text{C}_6\text{H}_4\text{NO}_2\text{-4}$) (2 mmol) in 50 mL of methanol was heated under reflux for 30 min. The resulting solution was evaporated to dryness, and the solid residue was dissolved in dichloromethane (ca. 20 mL) and filtered into stirred diethyl ether (ca. 100 mL) to give a brown solid precipitate. The resulting solid was washed with diethyl ether (2×20 mL), dissolved in dichloromethane (ca. 25 mL), and treated, at room temperature, with Al_2O_3 (for complex **4**; 1.019 g, 10 mmol) or K_2CO_3 (for complex **5**; 1.382 g, 10 mmol) for 1 h. The solution was then evaporated to dryness, and the residue was extracted with diethyl ether. The evaporation of the diethyl ether gave **4** and **5** as red solids. Yield, IR (KBr, $\nu(\text{C}\equiv\text{C})$, cm^{-1}), and analytical or mass spectral data (FAB m/e) are as follows. For **4**. 60% (0.592 g). 2070, 2207. Anal. Calcd for $\text{RuC}_{61}\text{H}_{45}\text{P}_2\text{O}_2\text{N}$: C, 74.22; H, 4.59; N, 1.41. Found: C, 73.85; H, 4.22; N, 1.30. For **5**. 51% (0.505 g). 2069. MS for $\text{RuC}_{60}\text{H}_{46}\text{P}_2\text{O}_2\text{N}_2$: $[\text{M}^+] = 990$, $[\text{M}^+ - \text{PPh}_3] = 728$.

Synthesis of $[\text{Ru}\{\text{C}\equiv\text{CCH}_2(\text{PPh}_3)\}_2(\eta^5\text{-C}_9\text{H}_7)(\text{PPh}_3)_2][\text{PF}_6]$ (6**).** A mixture of $[\text{RuCl}(\eta^5\text{-C}_9\text{H}_7)(\text{PPh}_3)_2]$ (**1a**) (0.776 g, 1 mmol), NaPF_6 (0.336 g, 2 mmol), $\text{HC}\equiv\text{CCH}_2(\text{OH})$ (0.118 mL, 2 mmol), and PPh_3 (2.622 g, 10 mmol) in 50 mL of methanol was stirred at room temperature for 8 h. A yellow suspension was formed. The solvent was then decanted, and the solid residue was dissolved in dichloromethane (ca. 40 mL) and filtered over kieselguhr. The resulting solution was evaporated to dryness, and the yellow solid obtained was washed with diethyl ether (2×20 mL) and vacuum-dried. Yield, IR (KBr, $\nu(\text{PF}_6^-)$, $\nu(\text{C}\equiv\text{C})$, cm^{-1}), analytical, and NMR spectroscopic data (ppm) are as follows. 65% (0.771 g). 837, 2087. Anal. Calcd for $\text{RuC}_{66}\text{H}_{54}\text{F}_6\text{P}_4$: C, 66.83; H, 4.59. Found: C, 67.11; H, 4.69. $^{31}\text{P}\{^1\text{H}\}$ ($(\text{CD}_3)_2\text{CO}$) δ 18.51 (t, $^5J_{\text{PP}} = 4.6$ Hz, $\text{CH}_2\text{-PPh}_3$), 51.32 (d, $^5J_{\text{PP}} = 4.6$ Hz, Ru-PPh_3); ^1H ($(\text{CD}_3)_2\text{CO}$) δ 4.40 (d, 2H, J_{HH}

$= 2.3$ Hz, H-1,3), 4.82 (t, 1H, $J_{\text{HH}} = 2.3$ Hz, H-2), 4.91 (d, 2H, $^2J_{\text{HP}} = 14.5$ Hz, CH_2), 6.07 and 6.84 (m, 2H each one, H-4,7 and H-5,6), 7.07–8.06 (m, 45H, Ph); $^{13}\text{C}\{^1\text{H}\}$ ($(\text{CD}_3)_2\text{CO}$) δ 21.39 (d, $J_{\text{CP}} = 54.2$ Hz, CH_2), 74.84 (s, C-1,3), 93.03 (d, $^2J_{\text{CP}} = 12.2$ Hz, C_β), 95.46 (s, C-2), 110.15 (s, C-3a,7a), 111.38 (m, Ru-C_α), 119.85–139.60 (m, Ph, C-4,7 and C-5,6); $\Delta\delta(\text{C-3a,7a}) = -20.55$.

Synthesis of $[\text{Ru}\{\text{C}\equiv\text{CCH}=\text{CH}(\text{CH}=\text{CH})_n\text{R}\}_2(\eta^5\text{-C}_9\text{H}_7)(\text{PPh}_3)_2]$ ($n = 0$, $\text{R} = \text{C}_6\text{H}_4\text{NO}_2\text{-4}$ [(*E,Z*)-7a**], $\text{C}_4\text{H}_2\text{ONO}_2\text{-2,3}$ [(*E,Z*)-**8a**], $\text{C}_4\text{H}_2\text{SNO}_2\text{-2,3}$ [(*E*)-**8b**], $\text{C}_6\text{H}_4\text{CN-4}$ [(*E,Z*)-**13**], $\text{C}_5\text{H}_4\text{N-4}$ [(*E*)-**16**], $\text{C}_5\text{H}_4\text{FeC}_5\text{H}_5$ [(*E*)-**18**]; $n = 1$, $\text{R} = \text{C}_6\text{H}_4\text{NO}_2\text{-4}$ [(*EE,ZE*)-**7b**]), and $[\text{Ru}\{\text{C}\equiv\text{CCH}=(\text{C}_6\text{H}_4\text{NO}_2\text{-3})_2\}(\eta^5\text{-C}_9\text{H}_7)(\text{PPh}_3)_2]$ (**9**).** General Procedure. A solution of Li^iBu (1.6 M in hexane, 0.625 mL, 1 mmol) was added to a solution of $[\text{Ru}\{\text{C}\equiv\text{CCH}_2(\text{PPh}_3)\}_2(\eta^5\text{-C}_9\text{H}_7)(\text{PPh}_3)_2][\text{PF}_6]$ (**6**) (1.186 g, 1 mmol) in 25 mL of THF kept at -20 °C. After the addition was complete, the color of the solution had changed from yellow to violet. After stirring the resulting mixture for 15 min, the corresponding aldehyde or ketone (3 mmol) was added and stirred for 30 min after warming to room temperature. The solvent was then removed in vacuo, and the solid residue was transferred to an Alox I chromatography column. Elution with hexane/diethyl ether (3/1) gave an orange band from which the corresponding σ -enynyl complex was obtained by solvent removal. Yield, IR (KBr, $\nu(\text{C}\equiv\text{C})$, $\nu(\text{C}\equiv\text{N})$, cm^{-1}), and analytical or mass spectral data (FAB m/e) are as follows. For **7a**. 90% (0.822 g). 2034 (*E* and *Z* isomers). Anal. Calcd for $\text{RuC}_{55}\text{H}_{43}\text{O}_2\text{P}_2\text{N}$: C, 72.35; H, 4.75; N, 1.53. Found: C, 71.89; H, 4.96; N, 1.36. For **7b**. 73% (0.685 g). 2033 (*EE* and *ZE* isomers). Anal. Calcd for $\text{RuC}_{57}\text{H}_{45}\text{O}_2\text{P}_2\text{N}$: C, 72.91; H, 4.83; N, 1.49. Found: C, 72.91; H, 4.88; N, 1.42. For **8a**. 41% (0.370 g). 2027 (*E* and *Z* isomers). MS for $\text{RuC}_{53}\text{H}_{41}\text{O}_3\text{P}_2\text{N}$: $[\text{M}^+] = 903$, $[\text{M}^+ - \text{PPh}_3] = 642$. For **8b**. 46% (0.423 g). 2021. MS for $\text{RuC}_{53}\text{H}_{41}\text{O}_2\text{P}_2\text{NS}$: $[\text{M}^+] = 919$, $[\text{M}^+ - \text{PPh}_3] = 657$. For **9**. 88% (0.909 g). 2034. Anal. Calcd for $\text{RuC}_{61}\text{H}_{46}\text{O}_4\text{P}_2\text{N}_2$: C, 70.85; H, 4.48; N, 2.70. Found: C, 70.25; H, 4.82; N, 2.58. For **13**. 71% (0.634 g). 2041 ($\text{C}\equiv\text{C}$, *E* and *Z* isomers), 2216 ($\text{C}\equiv\text{N}$, *E* isomer), 2137 ($\text{C}\equiv\text{N}$, *Z* isomer). Anal. Calcd for $\text{RuC}_{56}\text{H}_{43}\text{P}_2\text{N}$: C, 75.32; H, 4.85; N, 1.56. Found: C, 74.59; H, 5.01; N, 1.49. For **16**. 83% (0.721 g). 2039. Anal. Calcd for $\text{RuC}_{54}\text{H}_{43}\text{P}_2\text{N}$: C, 74.55; H, 4.98; N, 1.61. Found: C, 73.95; H, 4.62; N, 1.58. For **18**. 67% (0.654 g). 2048. Anal. Calcd for $\text{FeRuC}_{59}\text{H}_{48}\text{P}_2$: C, 72.61; H, 4.96. Found: C, 72.36; H, 4.93.

Synthesis of $[\text{Ru}(\text{C}\equiv\text{N})(\eta^5\text{-C}_9\text{H}_7)(\text{PPh}_3)_2]$ (10**).** A mixture of $[\text{RuCl}(\eta^5\text{-C}_9\text{H}_7)(\text{PPh}_3)_2]$ (**1a**) (0.776 g, 1 mmol), and KCN (0.260 g, 4 mmol) in 50 mL of methanol was heated under reflux for 1 h. The resulting solution was concentrated (ca. 20 mL) to give, after cooling to -10 °C, yellow crystals of complex **10**. Yield, IR (KBr, $\nu(\text{C}\equiv\text{N})$, cm^{-1}), analytical, and NMR spectroscopic data (ppm) are as follows. 81% (0.767 g). 2071. Anal. Calcd for $\text{RuC}_{46}\text{H}_{37}\text{P}_2\text{N}$: C, 72.05; H, 4.86; N, 1.82. Found: C, 71.35; H, 4.91; N, 1.72. $^{31}\text{P}\{^1\text{H}\}$ (CD_2Cl_2) δ 51.94 (s); ^1H (CD_2Cl_2) δ 4.57 (d, 2H, $J_{\text{HH}} = 2.5$ Hz, H-1,3), 5.17 (t, 1H, $J_{\text{HH}} = 2.5$ Hz, H-2), 6.45 and 6.90 (m, 2H each one, H-4,7 and H-5,6), 7.13–7.69 (m, 30H, Ph); $^{13}\text{C}\{^1\text{H}\}$ (CD_2Cl_2) δ 73.87 (s, C-1,3), 94.43 (s, C-2), 109.26 (s, C-3a,7a), 123.89 (s, C-4,7 or C-5,6), 127.45–137.61 (m, Ph and C-4,7 or C-5,6), 143.49 (t, $^2J_{\text{CP}} = 22.7$ Hz, $\text{Ru-C}\equiv\text{N}$); $\Delta\delta(\text{C-3a,7a}) = -21.44$.

Synthesis of $[(\eta^5\text{-C}_9\text{H}_7)(\text{PPh}_3)_2\text{Ru}\{\mu\text{-C}\equiv\text{N}\}\text{M}(\text{CO})_5]$ ($\text{M} = \text{Cr}$ (11a**), W (**11b**)), $[(\eta^5\text{-C}_9\text{H}_7)(\text{PPh}_3)_2\text{Ru}\{\mu\text{-C}\equiv\text{CCH}=\text{CH}-\text{C}_6\text{H}_4\text{C}\equiv\text{N-4}\}\text{M}(\text{CO})_5]$ ($\text{M} = \text{Cr}$ [(*E,Z*)-**14a**], W [(*E,Z*)-**14b**]), and $[(\eta^5\text{-C}_9\text{H}_7)(\text{PPh}_3)_2\text{Ru}\{\mu\text{-C}\equiv\text{CCH}=\text{CH}-\text{C}_5\text{H}_4\text{N-4}\}\text{M}(\text{CO})_5]$ ($\text{M} = \text{Cr}$ [(*E*)-**17a**], W [(*E*)-**17b**]).** General Procedure. A solution of **10**, (*E,Z*)-**13** or (*E*)-**16** (1 mmol) in 25 mL of THF was treated with a THF solution of $[\text{M}(\text{CO})_5\text{-}(\text{THF})]$ ($\text{M} = \text{Cr}$, W) (1 mmol), and the mixture was stirred at room temperature for 1 h. The solution was then evaporated to dryness, and the orange solid residue was washed with hexane (ca. 10 mL). Yield, IR (KBr, $\nu(\text{C}\equiv\text{C})$, $\nu(\text{C}\equiv\text{O})$, $\nu(\text{C}\equiv\text{N})$, cm^{-1}), analytical, and NMR spectroscopic data (ppm) are as follows. For **11a**. 70% (0.678 g). 1884, 1930, 2064, 2109. Anal.

Calcd for CrRuC₅₁H₃₇O₅P₂N: C, 63.88; H, 3.89; N, 1.46. Found: C, 64.34; H, 4.18; N, 1.43. ³¹P{¹H} (CD₂Cl₂) δ 54.61 (s); ¹H (CD₂Cl₂) δ 4.34 (d, 2H, J_{HH} = 1.5 Hz, H-1,3), 4.46 (t, 1H, J_{HH} = 1.5 Hz, H-2), 6.67 and 6.79 (m, 2H each one, H-4,7 and H-5,6), 6.92–7.75 (m, 30H, Ph); ¹³C{¹H} (CD₂Cl₂) δ 74.61 (s, C-1,3), 92.52 (s, C-2), 107.95 (s, C-3a,7a), 123.66 (s, C-4,7 or C-5,6), 127.80–136.93 (m, Ph and C-4,7 or C-5,6), 155.97 (t, ²J_{CP} = 20.7 Hz, Ru–C≡N), 216.02 and 220.76 (s, C=O); Δδ(C-3a,7a) = –22.75. For **11b**. 85% (0.927 g). 1881, 1922, 2065, 2099. Anal. Calcd for RuWC₅₁H₃₇O₅P₂N: C, 56.16; H, 3.42; N, 1.28. Found: C, 55.96; H, 3.65; N, 1.22. ³¹P{¹H} (CD₂-Cl₂) δ 54.19 (s); ¹H (CD₂Cl₂) δ 4.52 (d, 2H, J_{HH} = 2.4 Hz, H-1,3), 4.66 (t, 1H, J_{HH} = 2.4 Hz, H-2), 6.73 and 6.93 (m, 2H each one, H-4,7 and H-5,6), 7.18–7.70 (m, 30H, Ph); ¹³C{¹H} (CD₂-Cl₂) δ 75.12 (s, C-1,3), 92.56 (s, C-2), 107.81 (s, C-3a,7a), 123.62 (s, C-4,7 or C-5,6), 127.71–136.93 (m, Ph and C-4,7 or C-5,6), 154.80 (t, ²J_{CP} = 20.6 Hz, Ru–C≡N), 198.18 and 201.84 (s, C=O); Δδ(C-3a,7a) = –22.89. For **14a**. 76% (0.825 g). 1909, 1946, 2041, 2073, 2220 (*E* and *Z* isomers). Anal. Calcd for CrRuC₆₁H₄₃O₅P₂N: C, 67.52; H, 3.99; N, 1.29. Found: C, 67.72; H, 3.87; N, 1.35. For **14b**. 82% (0.999 g). 1907, 1980, 2039, 2074, 2221, 2232 (*E* and *Z* isomers). Anal. Calcd for RuWC₆₁H₄₃O₅P₂N: C, 60.21; H, 3.56; N, 1.15. Found: C, 59.84; H, 3.41; N, 1.20. For **17a**. 70% (0.743 g). 1896, 1933, 2036, 2065. Anal. Calcd for CrRuC₅₉H₄₃O₅P₂N: C, 66.79; H, 4.08; N, 1.32. Found: C, 66.82; H, 3.97; N, 1.26. For **17b**. 85% (1.014 g). 1896, 1927, 2034, 2069. Anal. Calcd for RuWC₅₉H₄₃O₅P₂N: C, 59.41; H, 3.63; N, 1.17. Found: C, 60.05; H, 3.83; N, 1.09.

Synthesis of [(η⁵-C₉H₇)(PPh₃)₂Ru(μ-C≡N)Ru(NH₃)₅][CF₃SO₃]₃ (12**) and [(η⁵-C₉H₇)(PPh₃)₂Ru(μ-C≡CCH=CH-C₆H₄C≡N-4)Ru(NH₃)₅][CF₃SO₃]₃ [(*E*, *Z*)-**15**]. **General Procedure.** A solution of complex **10** or (*E*, *Z*)-**13** (1 mmol) in 20 mL of acetone was treated with [Ru(NH₃)₅(OSO₂CF₃)]₂[CF₃SO₃]₂ (0.633 g, 1 mmol), and the mixture was stirred at room temperature for 1 h. The solution was then concentrated (ca. 5 mL). The slow addition of diethyl ether (ca. 25 mL) allowed the formation of a biphasic system affords, after 24 h, blue crystals of **12** or red crystals of (*E*, *Z*)-**15**. Yield, IR (KBr, ν(C≡N), ν(C≡C), ν(NH₃), cm⁻¹), analytical, and conductivity (acetone, Ω⁻¹ cm² mol⁻¹) data are as follows. For **12**. 79% (1.106 g). 2006, 3314. Anal. Calcd for Ru₂C₄₉H₅₂F₉O₉N₆S₃P₂: C, 42.03; H, 3.74; N, 6.00. Found: C, 41.44; H, 4.04; N, 5.30. 209. For **15**. 53% (0.809 g). 2037, (C≡C *E* and *Z* isomers), 2190 (C≡N, *E* isomer), 2222 (C≡N, *Z* isomer), 3308 (NH₃, *E* and *Z* isomers). Anal. Calcd for Ru₂C₅₉H₅₈F₉O₉N₆S₃P₂: C, 46.43; H, 3.83; N, 5.50. Found: C, 46.24; H, 3.78; N, 5.54. 215.**

Synthesis of [Ru{=C=C(H)CH=CHC₅H₄FeC₅H₅}(η⁵-C₉H₇)(PPh₃)₂][BF₄]₂ [(*E*)-19**]. A solution of HBF₄·Et₂O (1.9 mL, 1.5 mmol) in 10 mL of diethyl ether was added dropwise, at –20 °C, to a solution of complex (*E*)-**18** (0.976 g, 1 mmol) in 30 mL of THF. The reaction mixture was gradually warmed to room temperature and then concentrated (ca. 5 mL). Addition of diethyl ether (ca. 100 mL) gave complex (*E*)-**19** as a brown solid which was washed with diethyl ether (3 × 20 mL) and vacuum-dried. Yield, IR (KBr, ν(BF₄⁻), cm⁻¹), analytical data, conductivity (acetone, Ω⁻¹ cm² mol⁻¹), and NMR spectroscopic data (ppm) are as follows. 71% (1.064 g). 1060. Anal. Calcd for FeRuC₅₉H₄₉F₄P₂B₂: C, 66.62; H, 4.64. Found: C, 65.91; H, 4.89. 110. ³¹P{¹H} (CD₂Cl₂) δ 40.60 (s); ¹H (CD₂-Cl₂) δ 4.14 (s, 5H, C₅H₅), 4.23 and 4.30 (m, 2H each one, C₅H₄), 5.34 (bs, 1H, Ru=C=CH), 5.52 (d, 2H, J_{HH} = 2.4 Hz, H-1,3), 5.72 (t, 1H, J_{HH} = 2.4 Hz, H-2), 5.82 (d, 1H, J_{HH} = 15.2 Hz, =CH), 6.15 (m, 2H, H-4,7 or H-5,6), 6.89–7.54 (m, 33H, Ph, =CH and H-4,7 or H-5,6); ¹³C{¹H} (CD₂Cl₂) δ 66.99 and 69.84 (s, CH of C₅H₄), 70.34 (s, C₅H₅), 84.75 (s, C-1,3), 95.41 (s, C of C₅H₄), 98.98 (s, C-2), 108.34 and 124.28 (s, =CH), 115.53 (s, C-3a,7a), 118.55 (s, C_β), 123.43 and 130.70 (s, C-4,7 and C-5,6), 128.96–134.18 (m, Ph), 361.82 (t, ²J_{CP} = 16.5 Hz, Ru=C_α); Δδ(C-3a,7a) = –15.17.**

HRS Measurements. IR laser pulses generated with an injection-seeded Q-switched Nd:YAG laser (Quanta-Ray GCR-

5, 1064 nm, 10 ns pulses, 10 Hz) were focused into a cylindrical cell (7 mL) containing the sample. The fundamental intensity was altered by rotation of a half-wave plate placed between crossed polarizers and measured with a photodiode. An efficient condenser system was used to collect the light scattered at the harmonic frequency (532 nm) that was detected by a photomultiplier. Discrimination of the second-harmonic light from the fundamental light was accomplished by a low-pass filter and a 532-nm interference filter. Actual values for the intensities were retrieved by using gated integrators. In all experiments, the incident light was vertically polarized along the *z* axis. All HRS measurements were performed in dichloromethane, and the known hyperpolarizability of *p*-nitroaniline in this solvent was used as a reference.²⁹ The samples were passed through a 0.45-μm filter (contaminated samples often produce spurious signals), and were checked for multiphoton fluorescence that can interfere with the HRS signal.³⁰ Further details of the experimental procedure have been reported elsewhere.³¹

X-ray Diffraction Studies. X-ray suitable single crystals were obtained by slow diffusion of pentane into THF solutions of **7b** and **9**. Data collection, crystal, and refinement parameters are collected in Table 5. Data were collected with the ω–2θ scan technique and a variable scan rate, with a maximum scan time of 60 s per reflection. Atomic scattering factors were taken from International Tables for X-ray Crystallography (1974).³² Geometrical calculations were made with PARST97.³³ The crystallographic plots were made with EUCLID.³⁴ All calculations were made at the University of Oviedo on the X-ray group ALPHA-AXP computers.

Complex (EE)-7b. Crystals contain one molecule of THF and one of *n*-pentane. The unit cell parameters were obtained from the least-squares fit of 25 reflections (with θ between 6° and 11°). The final drift correction factors were between 0.99 and 1.05. On all reflections, profile analysis³⁵ was performed. Lorentz and polarization corrections were applied and the data were reduced to |F_o|² values.

The structure was solved by DIRDIF-96³⁶ (Patterson methods and phase expansion). Isotropic full-matrix least-squares refinement on |F_o|² using SHELXL93³⁷ was performed.

Finally, all hydrogen atoms were geometrically placed. During the final stages of the refinement, the positional parameters and the anisotropic thermal parameters of most non-H-atoms were refined. Some C-atoms were isotropically refined because of the thermal parameters were out of physical meaning. The geometrically placed hydrogen atoms were isotropically refined, riding on their parent atoms. Two highly

(29) Stähelin, M.; Burland, D. M.; Rice, J. E. *Chem. Phys. Lett.* **1992**, *191*, 245.

(30) (a) Hendricks, E.; Dehu, C.; Clays, K.; Brédas, J. L.; Persoons, A. In *Polymers for Second-Order Nonlinear Optics*; ACS Symposium Series 601; Lindsay, G. A., Singer, K. D., Eds.; American Chemical Society: Washington, DC, 1995; p 82. (b) Flipse, M. C.; de Jonge, R.; Woudenberg, R. H.; Marsman, A. W.; van Walree, C. A.; Jennekens, L. W. *Chem. Phys. Lett.* **1995**, *245*, 297. (c) Morrison, I. D.; Denning, R. G.; Laidlaw, W. M.; Stammers, M. A. *Rev. Sci. Instrum.* **1996**, *67*, 1445.

(31) (a) Clays, K.; Persoons, A. *Rev. Sci. Instrum.* **1992**, *63*, 3285. (b) Houbrechts, S.; Clays, K.; Persoons, A.; Pikramenou, Z.; Lehn, J.-M. *Chem. Phys. Lett.* **1996**, *258*, 485.

(32) *International Tables for X-ray Crystallography*; Kynoch Press: Birmingham, U.K., 1974; Vol. IV.

(33) Nardelli, M. *Comput. Chem.* **1983**, *7*, 95.

(34) Spek, A. L. The EUCLID Package. In *Computational Crystallography*; Sayre D., Ed.; Clarendon Press: Oxford, U.K., 1982; p 528.

(35) (a) Grant, D. F.; Gabe, E. J. *J. Appl. Crystallogr.* **1978**, *11*, 114. (b) Lehman, M. S.; Larsen, F. K. *Acta Crystallogr., Sect. A* **1974**, *30*, 580.

(36) Beurskens, P. T.; Beurskens, G.; Bosman, W. P.; de Gelder, R.; Garcia-Granda, S.; Gould, R. O.; Israël, R.; M. Smits, J. M. The DIRDIF-96 Program System; Technical Report; Crystallography Laboratory, University of Nijmegen: Nijmegen, The Netherlands, 1996.

(37) Sheldrick, G. M. SHELXL93. In *Crystallographic Computing 6*; Flack, H. D., Parkanyi, P., Simon, K., Eds.; IUCr/Oxford University Press: Oxford, U.K., 1993; p 111.

Table 5. Crystallographic Data for the Complexes **9** and **7b**

complex	9	7b
formula	C ₆₉ H ₆₂ N ₂ O ₆ P ₂ Ru	C ₆₆ H ₆₅ NO ₃ P ₂ Ru
fw	1178.21	1083.20
cryst syst	triclinic	monoclinic
space group	P1	C2/c
a (Å)	11.710(3)	32.94(3)
b (Å)	14.977(6)	15.73(5)
c (Å)	18.136(6)	21.37(3)
a (deg)	65.40(3)	90
β (deg)	84.07(3)	96.46(5)
γ (deg)	81.02(3)	90
V (Å ³)	2854(2)	11004(38)
Z	2	8
calcd density (g cm ⁻³)	1.36	1.31
F(000)	1224	4528
radiation (λ, Å)	Mo Kα (0.710 73)	Mo Kα (0.710 73)
cryst size (mm)	0.20 × 0.20 × 0.13	0.26 × 0.13 × 0.20
temp (K)	293	293
monochromator	graphite cryst	graphite cryst
m (mm ⁻¹)	0.39	0.39
diffraction geom	ω – 2θ	ω – 2θ
θ range for data collection (deg)	1.24 – 22.98	1.24 – 24.98
index ranges for data collection	0 ≤ h ≤ 12 –16 ≤ k ≤ 16 –19 ≤ l ≤ 19	0 ≤ h ≤ 39 0 ≤ k ≤ 18 –25 ≤ l ≤ 25
no. of rflns measd	8214	9855
no. of indep rflns	7921	9674
no. of variables	667	486
agreement between equiv rflns ^a	0.084	0.46
final R factors (I > 2σ(I))	R1 = 0.094 wR2 = 0.224	R1 = 0.100 wR2 = 0.192
final R factors (all data)	R1 = 0.214 wR2 = 0.241	R1 = 0.520 wR2 = 0.351

$$^a R_{\text{int}} = \sum(I - \langle I \rangle) / \sum I.$$

disordered solvent molecules (pentane and THF) were found. For both solvent molecules, the non-H-atoms were geometrically fixed and isotropically refined. The H-atoms were geometrically placed riding on their parent atoms and isotropically refined with fixed temperature factors (1.2 times the temperature factor of the parent carbon). In an attempt to improve results, one new set of data (10067 reflections) was measured at 200 K from a different crystal. Unfortunately, no significant improvements were achieved.

The function minimized was $[\sum \omega(F_o^2 - F_c^2)^2 / \sum \omega(F_o^2)^2]^{1/2}$ ($\omega = 1/[\sigma^2(F_o^2) + (0.0964P)^2]$ where $P = (\max(F_o^2, 0) + 2F_c^2)/3$ with $\sigma^2(F_o^2)$ from counting statistics). The maximum shift to esd ratio in the last full-matrix least-squares cycle was 0.651. The final difference Fourier map showed no peaks higher than 0.67 eÅ⁻³ or deeper than –1.27 eÅ⁻³.

Complex 9. Crystals contain two molecules of THF. The unit cell parameters were obtained from the least-squares fit of 25 reflections (with θ between 4° and 10°). The final drift correction factors were between 1.00 and 1.05. Profile analysis³⁵ was performed on all reflections. Lorentz and polarization corrections were applied and the data were reduced to $|F_o|$ values.

The structure was solved by Patterson using the program SHELXS86³⁸ and expanded by DIRDIF.³⁹ Isotropic least-squares refinement was performed using SHELXL76.⁴⁰ At this stage an empirical absorption correction was applied using DIFABS.⁴¹

Hydrogen atoms were geometrically placed. During the final stages of the refinement, the positional parameters and the anisotropic thermal parameters of the non-H-atoms were refined. The geometrically placed hydrogen atoms were isotropically refined with a common thermal parameter, riding on their parent atoms. The two disordered THF solvent molecules were isotropically refined. Their hydrogen atoms were refined with a fixed (1.1 times the thermal parameter of the bonded carbon atom) thermal parameter.

Finally, a full-matrix least-squares refinement on $|F_o|^2$ was made using SHELXL93.³⁷ The function minimized was $[\sum \omega(F_o^2 - F_c^2)^2 / \sum \omega(F_o^2)^2]^{1/2}$ ($\omega = 1/[\sigma^2(F_o^2) + (0.1361P)^2]$ where $P = (\max(F_o^2, 0) + 2F_c^2)/3$ with $\sigma^2(F_o^2)$ from counting statistics). The maximum shift to esd ratio in the last full-matrix least-squares cycle was 0.010. The final difference Fourier map showed no peaks higher than 1.20 eÅ⁻³ (near the two disordered THF solvent molecules) or deeper than –1.81 eÅ⁻³.

Acknowledgment. This work was supported by the Dirección General de Investigación Científica y Técnica (Project PB96-0558), the EU (Human Capital Mobility Program, Project ERBCHRXT 940501), Fund and Scientific Research-Flanders (G.0308.96), the Belgian Government (IUAP-16), and the University of Leuven (GOA/1/95). We thank the Ministerio de Educación y Cultura (MEC) and the Fundación para la Investigación Científica y Técnica de Asturias (FICYT) for fellowships to S.C. and V.C., respectively. S.H. is a Postdoctoral Fellow and K.C. a Senior Research Associate of the Belgian National Fund for Scientific Research.

Supporting Information Available: Crystal structure data for (EE)-**7b** and **9**, including tables of atomic parameters, anisotropic thermal parameters, bond distances, and bond angles. Ordering information is given on any current masthead page.

OM980672M

(38) Sheldrick, G. M. SHELX86. In *Crystallographic Computing 3*; Sheldrick, G. M., Kruger, C., Goddard R., Eds.; Clarendon Press: Oxford, U.K., 1985; p 175.

(39) Beurskens, P. T.; Admiraal, G.; Beurskens, G.; Bosman, W. P.; Garcia-Granda, S.; Gould, R. O.; Smits, J. M. M.; Smykalla, C. The DIRDIF Program System; Technical Report; Crystallography Laboratory, University of Nijmegen: Nijmegen, The Netherlands, 1992.

(40) (a) Sheldrick, G. M. SHELXL76: *Program for Crystal Structure Determination*; University of Cambridge: Cambridge, U.K., 1976. (b) Van der Maelen Uria J. F. Ph.D. Thesis, University of Oviedo, 1991.

(41) Walker, N.; Stuart, D. *Acta Crystallogr., Sect. A* **1983**, *39*, 158.